Journal of Geological Society of Sri Lanka Vol. 16 (2014), 170-205
Professor P.G. Cooray Memorial Volume

PETROLOGY OF CHARNOCKITIC GRANULITES AND CALC-SILICATE GRANULITES FROM SOUTH-SOUTHEASTERN HIGHLAND COMPLEX OF SRI LANKA: FURTHER CONSTRAINTS FOR PHYSICO-CHEMICAL CONDITIONS OF THEIR METAMORPHIC EVOLUTION

BERNARD NIHAL PRAME* AND JANAKA AJITH PREMA

Geological Survey and Mines Bureau, 569, Epitamulla Road, Pitakotte, Sri Lanka

Corresponding Author: e-mail-bernardprame@yahoo.com

ABSTRACT

In southern and southeastern parts of the Highland Complex (HC) of Sri Lanka, garnetiferous charnockitic granulites of granitic-granodioritic and tonalitic-trondjhemitic compositions are ubiquitous. Minor amounts of calc-silicate rocks and marble are intercalated with these rocks particularly in the southeastern HC. These two lithologies provide unique opportunity to study the physical conditions and fluid regime of their granulite facies metamorphism in two different chemical systems. Mineral chemistry and petrology of thirty (30) charnockitic granulites and five (05) calc-silicate rocks were studied to constrain the P-T conditions of granulite facies metamorphism and understand the characteristics of fluid regime.

Phase equilibria in calc-silicate rocks clearly indicate that peak metamorphic temperatures were not less than 875°C. In contrast, garnet-orthopyroxene and garnet-clinopyroxene thermometry of charnockitic granulites yields a wide range of temperatures from 650°C to 900°C indicating gross re-setting of cations in some of the samples. Garnet-pyroxene geobarometry yields paleopressure estimates from about 7.5 kb in the southwestern (*Matara*) area to over 10 Kb in the boundary area of southeastern HC including *Kataragama* area. Thus, in conformity with previous studies in other parts of the HC there is a pressure gradient of about 3 Kb from western HC to eastern HC in the studied area.

In Mg-depleted charnockitic rocks, garnet coronas are formed at the expense of pyroxene and plagioclase while in calc-silicate rocks secondary garnet is formed at the expense of scapolite + wollastonite or wollastonite + plagioclase. Formation of secondary garnet in charnockitic granulites and calc-granulites as a mineral reaction product and exsolution of extremely iron-rich orthopyroxene (Fs_{95}) in Mg-depleted charnockitic rocks can be attributed to an early phase of near isobaric cooling. Mineral paragenesis and T-CO_2 diagrams imply that calc-silicate rocks from different localities had varying CO_2 activities (X_{CO2} from 0.2 to 0.5). One calc-silicate rock indicates even higher CO_2 activity. Oxygen fugacity calculations for charnockitic granulites also imply two different ranges of oxygen fugacity, rocks of granitic-granodioritic composition having relatively low f_{O2} values compared to those of tonalitic-trondjhemitic composition. This could be the result of marked difference of bulk X_{Fe} values in these two rock types. Varying X_{CO2} values in calc-granulites and contrasting f_{O2} values in two different pyroxene granulite types can be best explained by internal fluid buffering and therefore these findings are at odds with hypothesis that advocates pervasive fluid infiltration during granulite facies metamorphism.

Keywords: *Mineral reactions, Geothemo-barometry, P-T path, Highland Complex*

INTRODUCTION

Petrological studies of granulites may reveal valuable information on processes and physico-chemical conditions prevailed in the lower crust. Two highly useful lithologies in this context are garnet-pyroxene granulites and calc-granulites. Studies in which garnet-pyroxene-plagioclase-quartz assemblage has been employed to decipher P and T conditions and P-T-t path of

ancient lower crustal rocks are numerous (Hormann et al., 1980; Raith et al., 1983; Newton, 1983; Perkins and Chipera, 1985; Schumacher et al., 1990; Faulhaber and Raith, 1991). Though limited in numbers, studies based on calc-silicate assemblages are also on increase (Schenk, 1984; Warren et al., 1987; Harley and Buick, 1992; Harley et al., 1994; Bhowmik et al., 1995; Shaw and Arima, 1996; Sengupta et al., 1997). When these two types of lithologies are intercalated in a terrain, the possibility of constraining the peak P-T conditions, retrograde evolution and characterization of fluid regime are greatly enhanced as two independent sources of P-T-fluid information become available.

In southern and southeastern areas of the HC of Sri Lanka garnetiferous charnockitic pyroxene granulites are ubiquitous. Geological mapping has revealed that there are sporadically distributed thin marble bands and lenses or boudins of calc-silicate rocks intercalated with pyroxene granulites, particularly near the boundary between the Highland and Vijayan Complexes (Figure 1). These occurrences offer an opportunity to characterize the physico-chemical conditions of metamorphism using phase equilibria in two different chemical systems namely, Na_2O–CaO–K_2O–FeO–MgO–Al_2O_3–SiO_2 and CaO-MgO-FeO-Al_2O_3-SiO2. The present study-area (Figure 1) was selected mainly because of this reason, also considering the fact that the previous geothermobarometric surveys have largely excluded this part of the HC (Faulhaber and Raith, 1991; Schumacher and Faulhaber, 1994). As such, thirty (30) charnockitic pyroxene granulite samples, and five (05) calc-silicate rock samples from the southeastern HC of Sri Lanka were studied in order to understand P, T and fluid conditions of granulite facies metamorphism and characteristics of the P-T-t path of this part of the crust. Previous studies based on cation exchange thermometry of Grt-Px and Grt-Crd have produced a wide range of metamorphic temperatures for the HC. Therefore, one of the main objectives of this work was to bracket the peak metamorphic temperature of these rocks as

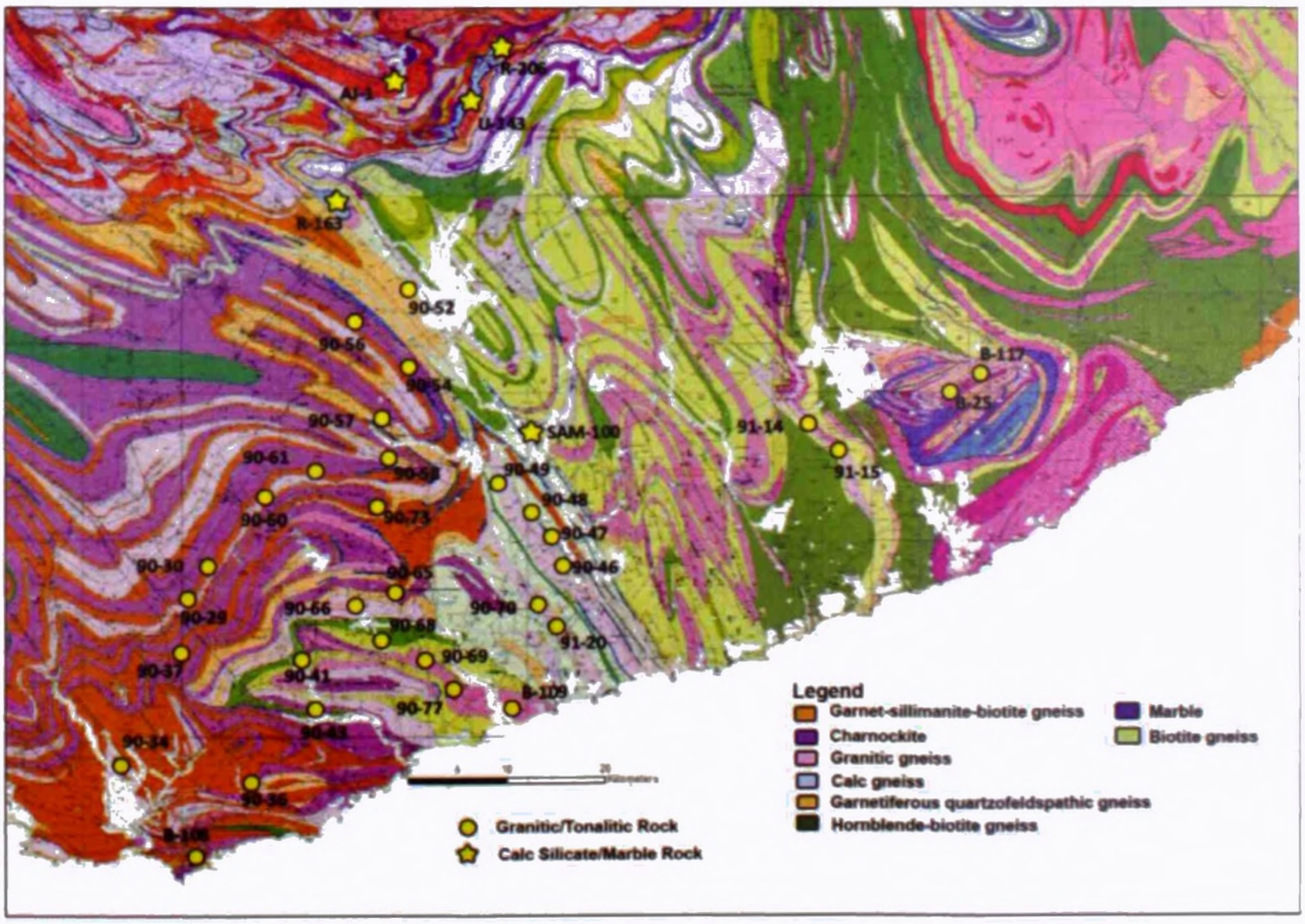

Fig. 1 Geological map of Southern and Southeastern Sri Lanka showing sample distribution

narrowly as possible.

GEOLOGICAL SETTING AND FIELD RELATIONS

Basement rocks of Sri Lanka are divided into three major lithotectonic units, namely the HC, the Vijayan Complex (VC) and the Wanni Complex (WC) (Milisenda et al., 1988; Cooray, 1994). The HC is mainly made up of highly metamorphosed supracrustal rocks and orthogneisses including charnockitic gneisses, charnockites and metabasites of which the Nd-model ages range from 2 to 3 Ga. (Kröner et al., 1991). The VC on right is a younger Nd-model age province (1-2 Ga) made up of hornblende-biotite gneisses and migmatitic gneisses, tectonically juxtaposed to the older HC (Kröner et al., 1991). WC on left is also a younger Nd-model age province but its lithology differs from VC in having some pelitic rocks and charnockitic rocks.

Study-area mostly covers the southernmost part of the HC dominated by granulite facies rocks. A few samples are from the granulite klippen within the amphibolite facies VC located east of the HC. Main rock types exposed in the area are charnockitic granitoids (pyroxene granulites) and garnetiferous quartzo-feldspathic rocks. Metabasite, metapelite and marble occur as minor constituents. Charnockitic rocks in the central HC are closely associated with typical metasedimentary marker beds such as quartzite, marble and garnet-sillimanite-graphite schist (khondalite). A marked difference between the central HC and the studied area is scarcity of such thick quartzite, marble and khondalite bands. Regional thermobarometric surveys have recorded higher paleo pressure estimates (~9 kb) in the eastern HC and lower values (~5 kb) in the westernmost parts (Faulharber and Raith, 1991; Schumacher et al., 1992; Prame, 1991). However, only a few samples from the southernmost part of the HC have been studied on previous occasions.

Geochemical studies show that most of the charnockitic granitoids in the area are of igneous origin (Prame, 1997). These granitoids now occurring as highly deformed bodies or layers were emplaced into the associated supracrustal sequence at various stages of the tectonic evolution, mostly between 1500-1900 Ma ago (Kröner and Williams, 1993; Hölzl et al., 1994). The original intrusive contacts were obscured by intense non-coaxial deformation associated with Pan-African metamorphism postulated by severe Pb-loss at some 590-610Ma ago (Kröner et al., 1994). Though detailed structural investigations have not yet been carried out in this area, field observations indicate that much of the structural interpretations employed to the central Highland Complex is valid in the study-area as well. Extreme stretching and isoclinal folding are the macro-scale evidence for earliest deformation. These isoclinal folds are re-folded into open folds. In fact, a system of early flat-lying isoclinal folds subsequently refolded into open to tight folds, is the most conspicuous structural feature in the central parts of the HC (Berger and Jayasinghe, 1976; Voll and Kleinschrodt, 1991). As shown in Figure 1, regional structural trends are mainly in NW-SE and WNW-ESE directions.

Charnockitic granitoids (pyroxene granulites) of the present study consist of two closely associated groups both occurring as discrete layers or deformed bodies (Prame, 1997). Rocks of granitic-adamellitic composition are commoner than tonalitic-trondjhemitic rocks which occur in subordinate amounts (Geological Map of Sri Lanka, 1982). These two groups of rocks are not distinguished in the existing geological maps as granitoids of different chemical affinities have been mapped as charnockite or charnockitic rocks. Prame, (1997) has shown that these charnockitic rocks of granitic and tonalitic-trondjhemitic composition have the chemical characteristics of A-type and I-type granitoids respectively. It appears that relatively minor layers of meta-tonalitic rocks are tectonically intercalated with layers or deformed bodies of granitic composition. Field evidences for relative age relations (intrusive) between these two groups have completely been obscured by strong flattening and stretching. Wollastonite-scapolite

bearing rocks have been reported from southwestern Sri Lanka where paleopressures around 6 kb have prevailed (Hapuarachchi, 1967; Hoffbauer and Spiering, 1994). During subsequent geological mapping of the southern and southeastern parts of the HC, a number of minor calc-silicate occurrences containing grossular, scapolite, diopside, wollastonite and ± anorthite have been noted (Geological sheet nos. 20 and 21, Geological Survey and Mines Bureau, Sri Lanka,). Wollastonite-scapolite-garnet granulites constitute only a very minor proportion (<1%) so that they cannot be shown as separate entities in the geological maps. These minor rocks have been overlooked or mapped as impure marble/calc-silicate rocks as they often occur as lenses, minor layers or boudins within marble (crystalline limestone). A study by Mathavan and Fernando (2001) first described the mineral reactions involving grossular, wollastonite and scapolite from this area.

METHOD OF STUDY AND ANALYTICAL TECHNIQUES

Thirty (30) polished thin sections were prepared from pyroxene-granulite samples collected from the areas that have been excluded in previous studies. Five (05) polished thin sections representative of five calc-silicate rocks intercalated with these rocks were also prepared. Most of the mineral analyses were performed on a Cameca Camebax (WDS) electron microprobe at the Mineralogical and Petrological Institute, Bonn University. The typical operating conditions were at15 KV and 15 nA probe current. Concentrations were calculated according to Pouchou and Pichoir (1984). A few analyses (sample U-143 and AJ-1) were obtained using JEOL Superprobe at the Chiba University.

RESULTS AND DISCUSSION

PYROXENE GRANULITES

PETROGRAPHY

Major mineral constituents of the studied pyroxene granulites samples are given in the Appendix Table 1. Common accessory minerals are ilmenite, apatite and zircon. Graphite, magnetite, sulphide minerals and alanite were observed in a few samples. Mineral abbreviations of Whitney and Evans (2010) were adopted whenever possible.

Following peak metamorphic assemblages were identified:

Grt+Opx+Cpx+Pl+Kfs+Qtz±Hbl±Bt
Grt+Opx+Pl+Kfs+Qtz±Hbl
Grt+Cpx+Pl+Kfs+Qtz±Hbl±Bt
Opx+Cpx+Pl+Kfs+Qtz±Hbl±Bt
Cpx+Pl+Kfs+Qtz±Hbl ±Bt

The above assemblages were encountered throughout the study-area typifying the granulite facies metamorphism. Textural features such as dimensional preferred orientations displayed by pyroxene and primary hornblende, stretched quartz, fractured and dislocated garnet, deformed twin lamellae in plagioclase indicate that these rocks have undergone penetrative (grain-scale) deformation. Garnet porphyroblasts and pyroxenes are set in a quartzo-feldspathic matrix. Clinopyroxene and plagioclase sometimes occur as inclusions of garnet. The granitic rocks from the *Kataragama* and *Kudaoya* klippen (B-25, B-117, 91-14) contain extremely stretched quartz ribbons occurring within a recrystallized polygonal feldspathic matrix exhibiting typical granulitic texture (Figure 2a; micromylonite?). Feldspar grains enclosed by quartz remains extremely stretched while matrix-feldspars have recrystallized into a granoblastic-polygonal texture. Sub-grain development of these stretched quartz is common. K-feldspar commonly occurs as microperthite but it occurs in the form of microcline in some retrogressed samples collected in the vicinity of HC/VC boundary area (91-15, 91-14, 90-46). K-feldspar is scarce in K- depleted tonalitic and trondjhemitic rocks. Though most garnet and orthopyroxene represent peak granulite facies metamorphism few samples contain garnet and orthopyroxene formed after peak conditions. In magnesium depleted (Fe/Fe+Mg) = 0.92-0.94

mol.) granitic-adamelletic samples (90-66, B-117, 90-25) orthopyroxene is of secondary origin while orthopyroxene is totally absent in samples that are extremely depleted in Mg (bulk Fe/Fe+Mg = 0.98 mol.; sample 91-14).

MINERAL REACTIONS

Two types of mineral reactions were observed in these pyroxene granulites. One reaction type produces secondary garnet at the expense of pyroxene and feldspar, while the other type indicates instability of garnet forming orthopyroxene and plagioclase bearing retrograde assemblages.

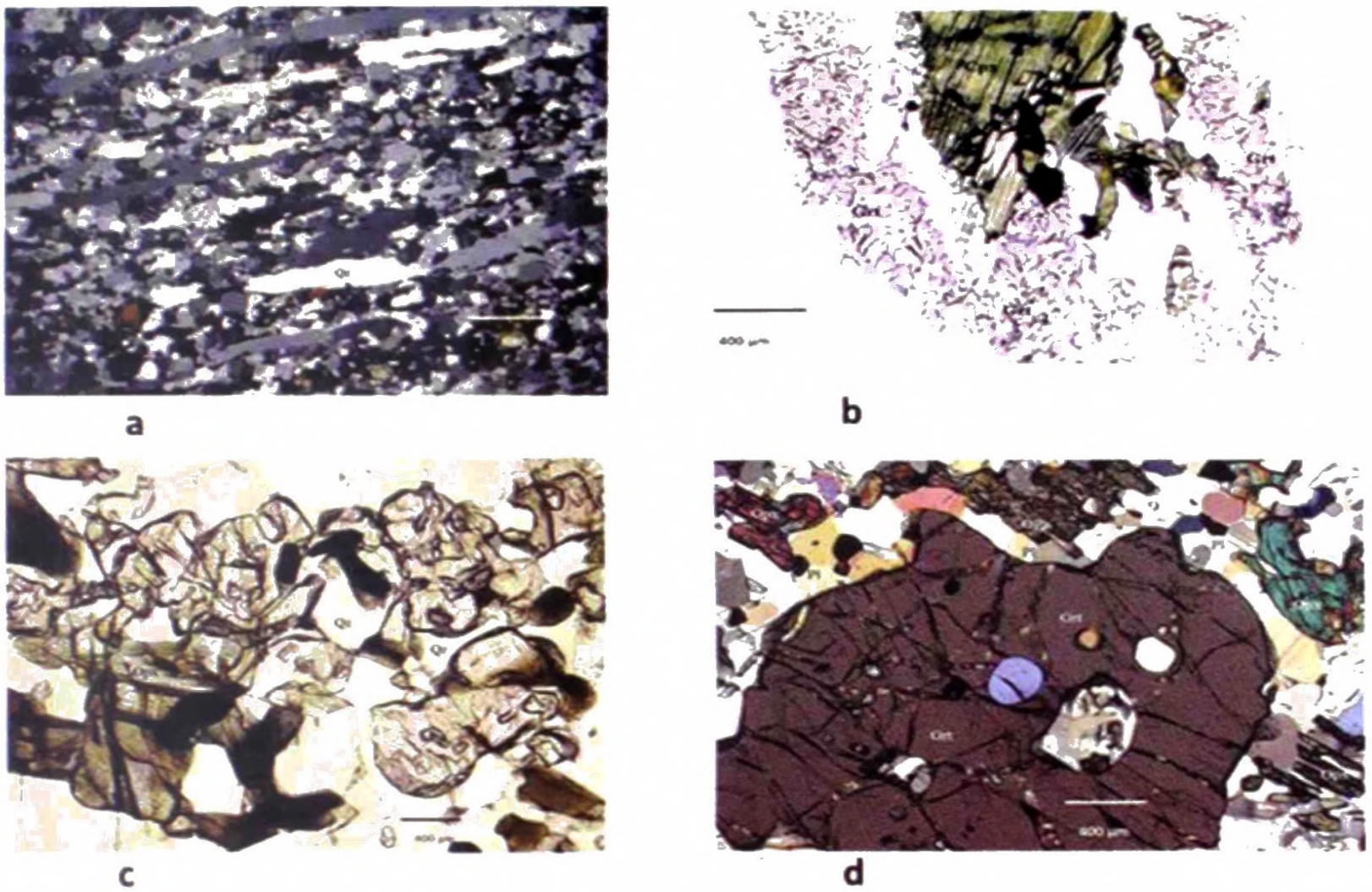

Fig. 2 (a) Extremely stretched quartz ribbons in a recrystallized polygonal feldspathic matrix (91-14). (b) Clinopyroxene grains surrounded by atolls of secondary garnet (B-117). Note that a part of post-deformational garnet ring runs perpendicular to the direction of preferred orientation of Cpx. (c) Garnet+quartz intergrowth associated with orthopyroxene and (d) Garnet porphyroblast (+ quartz) breaking down to form orthopyroxene and plagioclase (90-34).

The first type is particularly common in the Mg-depleted rocks of granitic composition occurring in the easternmost area. For example, high X_{Fe} granitic and adamellatic rocks Cpx grains are surrounded by atolls of secondary garnets, quartz and microperthite (Figure 2b). Plagioclase is rare in these rocks and therefore role of plagioclase in garnet producing reactions as a reactant is not explicit. Perhaps, this mineral has already been consumed or microperthite has acted as a source of Al and Ca. In fact, microperthite with corroded margins supports the latter contention. Therefore following model reactions can be proposed as the mechanism of garnet formation:

clinopyroxene + microperthite (An component)
→ garnet + quartz + opaques ---------- (1)

clinopyroxene + plagioclase (An component) →
garnet + quartz + opaques ---------- (2)

In the mm scale, garnet forms as rings around clinopyroxene cross-cutting the main L/S fabric. Formation of such retrograde garnet is usually attributed to an episode of near-isobaric cooling following peak metamorphism (e.g. Prame, 1991). In these high X_{Fe} samples orthopyroxene also being a retrograde mineral does not apparently contribute in garnet-forming reactions. As mentioned earlier, iron-rich orthopyroxene was initially an exsolved product

and then grew with further cooling. It is likely that they grew beyond the confines of the host Cpx after formation of garnet. In sample number 90-58, intergrowths of garnet and quartz replace orthopyroxene (Figure 2c) suggesting the reaction:

orthopyroxene + plagioclase → garnet + quartz -
----------(3)

Garnet and quartz intergrowths are aligned parallel to the preferred orientation of orthopyroxene however, they are clearly post-deformational.

Garnet pophyroblasts in samples 90-34 and 90-62 from the western part of the study-area breakdown to produce plagioclase and orthopyroxene (Figure. 2d) suggesting the reverse relationship;

garnet + quartz → orthopyroxene + plagioclase -
---------- (4)

Orthopyroxene partially mantled or replaced by hornblende or biotite (90-76, 91-20, 90-59) indicates hydration at a later stage.

PYROXENE EXSOLUTION AND FORMATION OF IRON RICH ORTHOPYROXENE

Clinopyroxene from granitic rocks and adamellitic rocks (90-66, B-117, B-25) with extremely high Fe/Fe+Mg mol. Ratios (0.80-0.98) display exsolution features that could probably explain the genesis of iron-rich orthopyroxene occurring in these rocks. Several grains of these pyroxenes were examined with polarizing microscope and back-scattered electron images to understand the process of exsolution. There are two optically discernible lamellae sets (Figures 3a, 3b). A set of very thin lamellae (thickness not more than few microns; from lower right to upper left) parallel to "001", at regular intervals is most conspicuous. The other set consists of slightly thicker (10-20 μm) lamellae (parallel "100"; from lower left to upper right) of iron rich Opx (Fs_{94}), spaced farther apart. These Opx lamellae have subsequently grown as rods (Figure 3a) beyond the confines of host Cpx. The apparent angle between the two sets is about 110°. Electron microprobe analyses on the thin "001" lamellae are inconsistent having the compositions similar to those on host Cpx ($Wo_{44}Fs_{52}En_4$) as well as pigeonite compositions . This may be due to the very fine nature of the lamellae. These "001" lamellae which were originally pigeonite but may have subsequently exsolved to Opx and Cpx . In Figure 3b, these lamellae patterns are depicted in a back scattered electron image. The grey coloured background is Cpx host. From upper left to lower right are thin "001" of which thickness does not exceed 2 μm. There is a segmentation of these lamellae by dark strips oriented parallel to"100" Opx lamellae (from lower left to upper right). Dark segments within "001" lamellae may represent fine exsolution lamellae or a set of dislocations/cavities. Also notable is the faulting of these "001" lamellae before the formation of iron-rich Opx lamellae. The Opx lamellae within Cpx should be parallel to "100" since this is the only plane of exact dimensional fit for both ortho- and clinopyroxene (Robinson, 1982). These microtextural features suggest that the exsolution process included following steps as proposed by Ollila et al. (1988); 1. Crystallization of homogeneous Cpx, 2. Exsolution of fine pigeonite lamellae parallel to "001", 3. faulting of pigeonite lamella and host Cpx along "100" and 4. formation of iron-rich Opx along the "100" with further cooling. Iron-rich orthopyroxene (Fs_{94}) now occurring as rods and laths associated with Cpx may have been initiated in this manner and grown with further cooling.

High temperature igneous lamellae are usually larger in size and fewer in number (Robinson, 1982). At low temperatures, a large number of lamellae may be initiated but because of slow diffusion rates they may only grow to very small sizes. Rather closely-spaced and very thin lamellae seen in these samples may have therefore exsolved below the peak temperature of granulite metamorphism. According to Lindsley (1983), pigeonite with X_{Fe} around 0.80 would be stable around 825°C at 9 Kb. However, formation of orthopyroxene lamellae and their growth may have taken place at well

below this temperature. Compositions of iron-rich orthopyroxene ($Fs_{94}Wo_3En_3$) and host Cpx give temperatures as low as 600°C (Lindsley, 1983) indicating advanced re-equilibration of cations between Cpx host and Opx that was in constant contact. However, temperature estimates obtained by employing the Grt-Opx thermometry using compositions of these Opx and secondary garnet in contact with each other are 640°C (using Harley, 1984) and 705°C (using Sen and Bhattacharya, 1984). Two pyroxene thermometers of Wells (1977) and Wood and Banno, (1973) yields temperatures around 775°C. These results indicate a minimum temperature of about 725°C for the formation of iron-rich orthopyroxene and at 700 °C, Fs_{94} wouldn't be stable below a pressure of 8 kb (Bohlen and Boettcher, 1981). The ideal conditions for stabilization and growth of this ferrosilite is substantial cooling at high pressure (isobaric cooling). In sample 90-66, isolated Cpx grains are absent. Cpx occurs as inclusions within iron-rich (Fs_{87}) Opx (Figure 3c). Cpx inclusions are in fact remnants of earlier Cpx host from which Opx have been exsolved. SEM image shows the extremely fine lamellae within Cpx and Opx (Figure 3d). Within these Cpx inclusions are lamellae which occasionally give sub-calcic compositions ($Wo_{33}Fe_{58}En_9$). This again indicates formation of pigeonite at an intermediate stage of pyroxene exsolution. A notable feature of the high-X_{Fe} rocks is the lack of primary Opx. This was most probably due to inadequate pressure condition to stabilize iron-rich Opx at peak metamorphic temperature. However, with subsequent cooling, favourable conditions for the formation of Opx may have prevailed.

GEOTHERMOBAROMETRY

Petrography and mineral chemistry of garnet-pyroxene granulites strongly indicate attainment of textural and chemical equilibrium during granulite facies metamorphism. However, as a response to subsequent cooling and unloading, inter-granular cation exchange and solid-solid mineral reactions took place in some local domains destroying the peak metamorphic equilibrium. Nevertheless, compositions of mineral porphyroblasts from unaffected samples or domains are most likely to represent the peak metamorphic conditions while the arrested mineral reactions and re-equilibrated domains may be useful to decipher the retrograde P-T trajectory. Ubiquitous garnet + orthopyroxene ± clinopyroxene + plagioclase + quartz assemblage allow the application of a number of geothermobarometers to the studied samples. For some calibrations involving pyroxenes, it was necessary to assign Fe^{+2} and Mg^{+2} to the M_3 and M_2 sites. Tetrahedral Al was taken as 2-Si and the remainder was assigned to M_3 (octahedral) site. Fe^{+3} was then calculated by charge balancing. M_3 and M_2 positions occupied by Fe^{+2} and Mg^{+2} were determined assigning Al^{+3}, Cr^{+3}, Ti^{+4}, Fe^{+3} to M_3 site and Ca^{+2}, Na^{+},Mn^{+2} to M_2 site. Then the available Fe^{+2} and Mg^{+2} were proportionally allocated to these two sites (Wood and Banno, 1973).

GEOTHERMOMETRY

Two geothermometers (Wood and Banno, 1973) based on Fe^{+2} and Mg^{+2} distribution between orthopyroxene and clinopyroxene and Lindsley (1983) were applied to 12 co-existing Opx-Cpx pairs at a nominal pressure of 8 kb (Appendix Table 7). The lowest temperatures; 688°C (Wood and Banno, 1973); 630°C (Lindsley,1983) are for sample 90-66 in which Cpx occurs as inclusions within the Opx. The low temperature may be due to advanced re-equilibration between Cpx inclusions and host Cpx. Temperatures for other samples vary from 742°C to 841°C (Wood and Banno, 1973) and from 670°C to 780°C (Lindsley,1983).

Temperature estimates from Grt-Opx (Harley, 1984; Sen and Bhattacharya, 1984) and Grt-Cpx (Ellis and Green, 1979) pairs are also presented in Appendix Table 7. Problems associated with the composition-activity relations of garnet introduce additional uncertainties in geothermometers involving with garnet and this has been clearly demonstrated by Faulhaber and Raith (1991) using a comprehensive set of Sri Lankan samples. The calibration of Harley

(1984) yields temperatures ranging from 638°C to 803°C which are generally lower than those obtained from Sen and Bhattacharya (1984) by about 100°C. Samples 90-117 and 90-66 which give lower temperatures (640°C and 700°C respectively) contain only secondary orthopyroxene. Sample 90-46 which yields a temperature of 638°C is also from a retrogressed quarry.

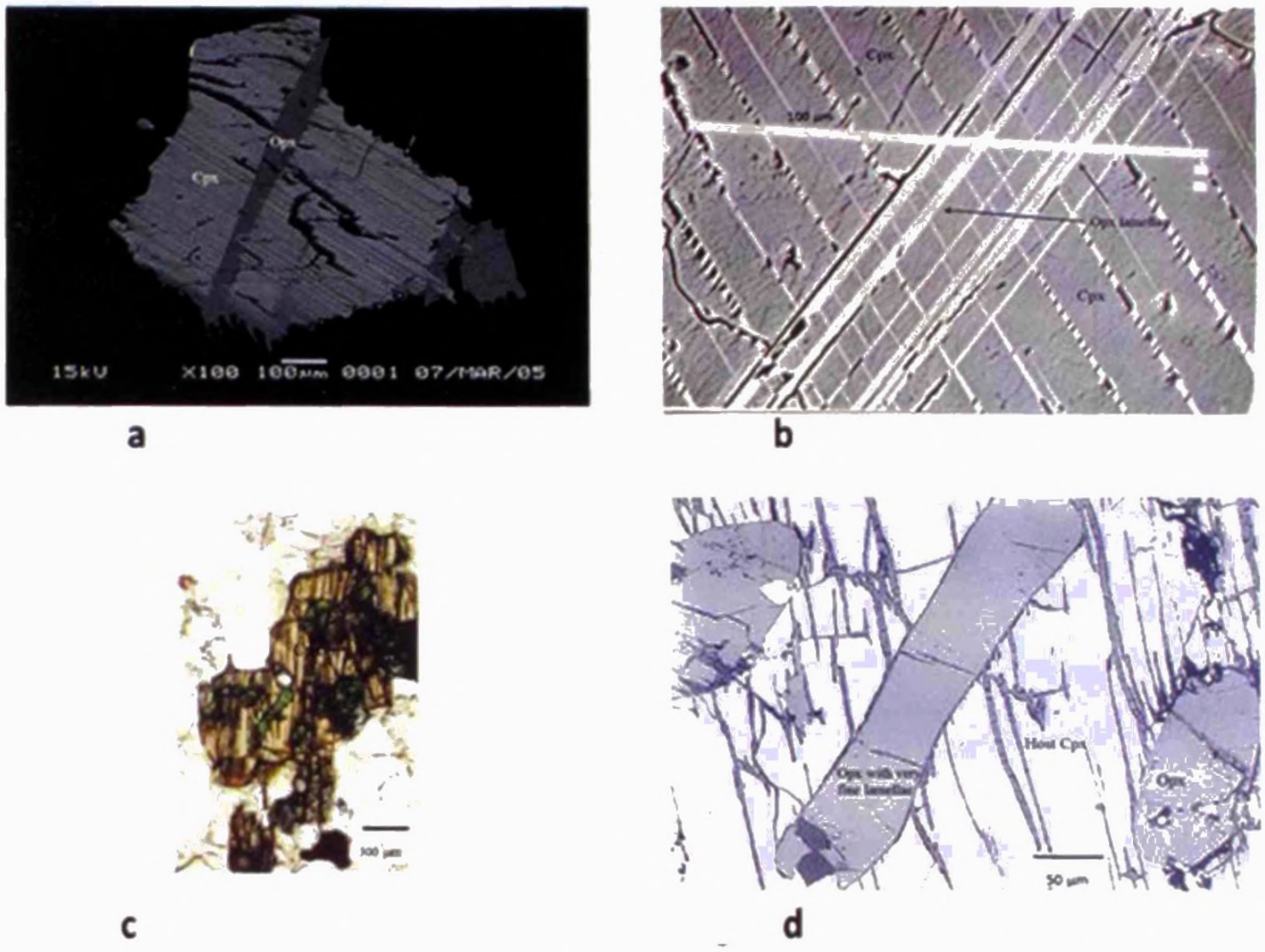

Fig. 3 (a) Exsolution lamellae of iron-rich clinopyroxene from granitoid rocks near Kataragama (B-25). (b) Back-scattered electron image depicting the exsolution phenomenon of iron-rich orthopyroxene. (c) Clinopyroxene inclusions (remnant?) in orthopyroxene host and (d) SEM image showing fine lamellae of Cpx inclusion and host Opx.

The temperature dependence of Fe^{+2} and Mg^{+2} distribution between coexisting garnet and clinopyroxene has been calibrated by several workers (Dahl, 1980; Raheim and Green, 1974; Ellis and Green, 1979). Experimental calibration of Ellis and Green (1979) was applied to 14 Grt-Cpx pairs (Appendix Table 7). These temperature estimates range from 733°C to 822°C but most of them are between 750°C and 775°C. There is less scatter in these temperatures, compared to the results obtained from Grt-Opx geothermometers. From the above discussion based on the Appendix Table 7 it is evident that the temperature estimates obtained from various calibrations scatter over a range between 662°C and 922°C (excluding retrogressed samples and samples with secondary Opx). There is no systematic regional variation of these temperatures.

GEOBAROMETRY

Geobarometers involving garnet+orthopyroxene +plagioclase+quartz assemblage have been widely applied to crustal rocks (Newton, 1983; Raith et al., 1983; Schumarcher et al., 1991). There are several formulations based on either measured thermodynamic data or experimental work (Perkins and Newton, 1981; Newton and Perkins, 1982; Bohlen et al., 1983; Perkins and Chipera, 1985; Berman, 1988; Bhattacharya et al., 1991).

Calibration by Newton and Perkins (1982) is based on measured thermodynamic data for the Mg end-member reaction (3) and inappropriate for the mostly iron-rich mineral compositions of

the present sample set ($X_{Fe\text{-}Opx}$ ranges from 0.45 to 0.95). Therefore, Fe end-member calibrations of Bhattacharya et al., (1991) and Perkins and Chipera (1985) were employed to calculate the palaeopressures. Pressures were also calculated using the thermodynamic data set of Holland and Powell (1998). Calculations were done at 800°C (Appendix Table 8) as most temperature estimates are between 750°C and 800°C, and also considering the fact that most of the thermochemcial data have been derived in this range of temperature. However, calculation for samples B-117 and 90-66 were made at 700°C as Opx in these two samples have been formed as a result of cooling.

Pressure estimates from Bhattacharya et al., (1991) are between 7 and 9.8 kb while the estimates from Perkins and Chipera (1995) are between 7.8 and 11 Kb (Appendix Table 8). For most of the samples there is a good agreement among the results obtained by different calibrations. Regional variations of the paleo-pressures calculated according to Perkins and Chipera (1985) is shown in Figure 5. A notable feature is that there is a pressure increase of 2-3 Kb from western parts towards the easternmost parts and *Kataragama* klippe, irrespective of the calibration employed. These results are compatible with the previous studies that indicated a pressure increase from west to east or southeast within the HC (Schumarcher et al., 1991) and confirms the paleopressure contouring by Faulhaber and Raith (1991). Thus, calculations at 800°C clearly indicate that the paleo-pressures in the southeastern part of the HC were not less than 10 kb.

In comparison to numerous studies based on Grt + Opx + Plag + Qtz geobarometer there is relatively fewer number of applications of Grt + Cpx + plag + qtz barometry (Perkins and Newton, 1981; Newton, 1982). Calibration by Newton and Perkins (1982) for the Cpx equilibria is based on Mg-end member reaction and therefore suitable for Mg-enriched mineral phases. Considering the ferriferous nature of the minerals encountered in the present study paleopressures were calculated at 800°C using thermochemical data set of Holland and Powell (1998).

In Appendix Table 8, results are compared with pressure estimates obtained from Grt + Opx + Pl + Qz barometer. At 800°C, there is excellent agreement between two barometers when applied to all (12) samples of two pyroxene granulite samples encountered in our study. Geographic distribution of the resultant pressures is also very much similar to that shown by Grt + Opx + pl + qz equilibria.

OPAQUE MINERALS AND OXIDIZING STATE OF CHARNOCKITIC ROCKS

Ilmenite is the dominant oxide mineral that occurs with or without graphite, pyrhotite or magnetite. Magnetite is restricted to tonalitic-trondhjemitic rocks which usually have relatively high Mg/Fe+Mg bulk compositions. Their ulvospinel component is less than 2% suggesting advanced re-equilibrium during cooling. Hematite component of ilmenite is also extremely low (<2%). These conclusions are based on optical examination and about 10 microprobe analyses (focussed beam-2-3 μm) of opaque phases per polished section. On rare occasions exsolution of Fe-Ti oxides were observed but reintegration of original compositions were not attempted as a detailed study of opaque phases and magnetic petrology of these samples is underway. The ilmenite+hedenbergite primary assemblage and hedenbergite+ferrosolite retrograde assemblage in high X_{Fe} charnockitic granulites implies a low oxygen fugacity with log f_{O2} values near or below the QFM buffer (Wones, 1989).

Despite advanced re-equilibration it may be possible to estimate oxygen fugacity using pyroxene-QUILF equilibria in the presence of two Fe-Ti oxides to estimate a maximum fo_2 value in the presence of ilmenite (Frost and Lindsley, 1992). Temperature calculated from two-oxide thermometry and two-pyroxene thermometry tally only for a few samples. In most cases oxide thermometry results in much lower temperatures indicating extreme resetting of cations in these minerals. Calculations yield

a range of oxygen fugacities from 10^{-12} to 10^{-20} bars. A notable feature is that charnockitic granitoids of granitic-adamellitic composition have the lower oxygen fugacities (10^{-14} – 10^{-20} bars) while granitoids of tonalitic-trondjhemititc compositions have relatively higher fugacities (10^{-12} - 10^{-16} bars). However, slightly higher oxygen fugacities might have prevailed in two types of lithologies during peak metamorphism. These observations suggest that the oxygen fugacitites of these rocks, buffered by silicate assemblage were fairly uniform throughout granitoid rocks having comparable X_{Fe}. Magnetic susceptibility measurements and available aeromagnetic anomaly maps also indicate the presence of relatively higher amount of magnetite in tonalitic and trondjhemitic rocks.

MINERAL CHEMISTRY

GARNET

Electron microprobe analyses of garnet cores from pyroxene granulite samples are presented in Appendix Table 2. The results show that these garnets essentially consist of almandine-grossular-pyrope solid solution. Almandine (Alm) content in granitic-ademalletic rocks is generally higher (65-74%) than that of tonalitic-trodhjemitic rocks (50-71%) and restricted to a narrow range. Pyrope (Prp) content which varies from 3 to 21% displays a reverse relationship. Grossular (Grs) component of all garnets is restricted to a very narrow range of 17-24%. Rim- interior- and core areas of selected garnet grains were probed in order to ascertain any compositional zoning. In most of the garnets there is no significant zoning penetrating into the grain interior except for local zoning of rims adjacent to plagioclase and ferromagnesian minerals. However, garnet in sample 91-14, particularly smaller grains show a significant zoning in Alm and Prp contents Alm and Prp contents increase towards the interior while spasertine (Sps) and Grs increase towards the rim. This type of zoning pattern can be developed after peak metamorphism due to resorption of outer part of the garnet (Tracy, 1982). Zoning of Alm and Sps was much more significant than that of Grs and Prp because no recipient minerals of Fe and Mn were involved in resorption.

ORTHOPYROXENE

Enstatite and ferrosilite components of orthopyroxene from 26 samples are presented in Appendix Table 3. Positive correlation between pyroxene composition (X_{Fe}) and bulk compositions is illustrated in Figure 4a. Two characteristic X_{Fe} ranges for granitic-adamellitic rocks and tonalitic-trondhjemitic rocks are also explicit in this diagram. Lower range (0.45-0.69) and higher range (0.68-0.93) of X_{Fe} corresponds to tonalitic and granitic rocks respectively. Magnesian-poor granitic rocks (91-14, 90-66, 90-117, B-25) contain orthopyroxene extremely rich in ferrosilite. In fact these have been exsolved and grown from clinopyroxene as a result of cooling. Bulk compositions of rocks containing ferrosilite rich orthopyroxene have been discussed and base on their high Fe/Fe+Mg values and other chemical characteristics these rocks have been classified as A-type anorogenic granitoids (Prame, 1997).

CLINOPYROXENE

Clnopyroxene was present in 15 rock samples and their compositions are given in Appendix Table 4. Their wollastonite and enstatite components vary from 42 to 46% and from 4 to 34% respectively. Thus they belong to diopside-hedenbergite series. These pyroxenes are very low in Al (0.035-0.08 p.f.u) and other non quadrilateral components. Electron microprobe analyses of certain points on lamellae of iron-rich Cpx (B-117) have given pigeonite compositions probably indicating the presence of fine Opx lamellae within these optically discernible lamellae. Dependence of X_{Fe} – Cpx on X_{Fe} - host rock is shown in Figure 4b.

PLAGIOCLASE

Plagioclase is an essential constituent in rocks of tonalitic to trondjhemitic composition. Its modal percentage is very low in granitic rocks occurring in the eastern parts (91-14, B-117). Plagioclase occurring in these rocks are low in An (14-20 %). An and Ab contents of plagioclase from 29 samples are presented in the Appendix Table 5. The variation of An content

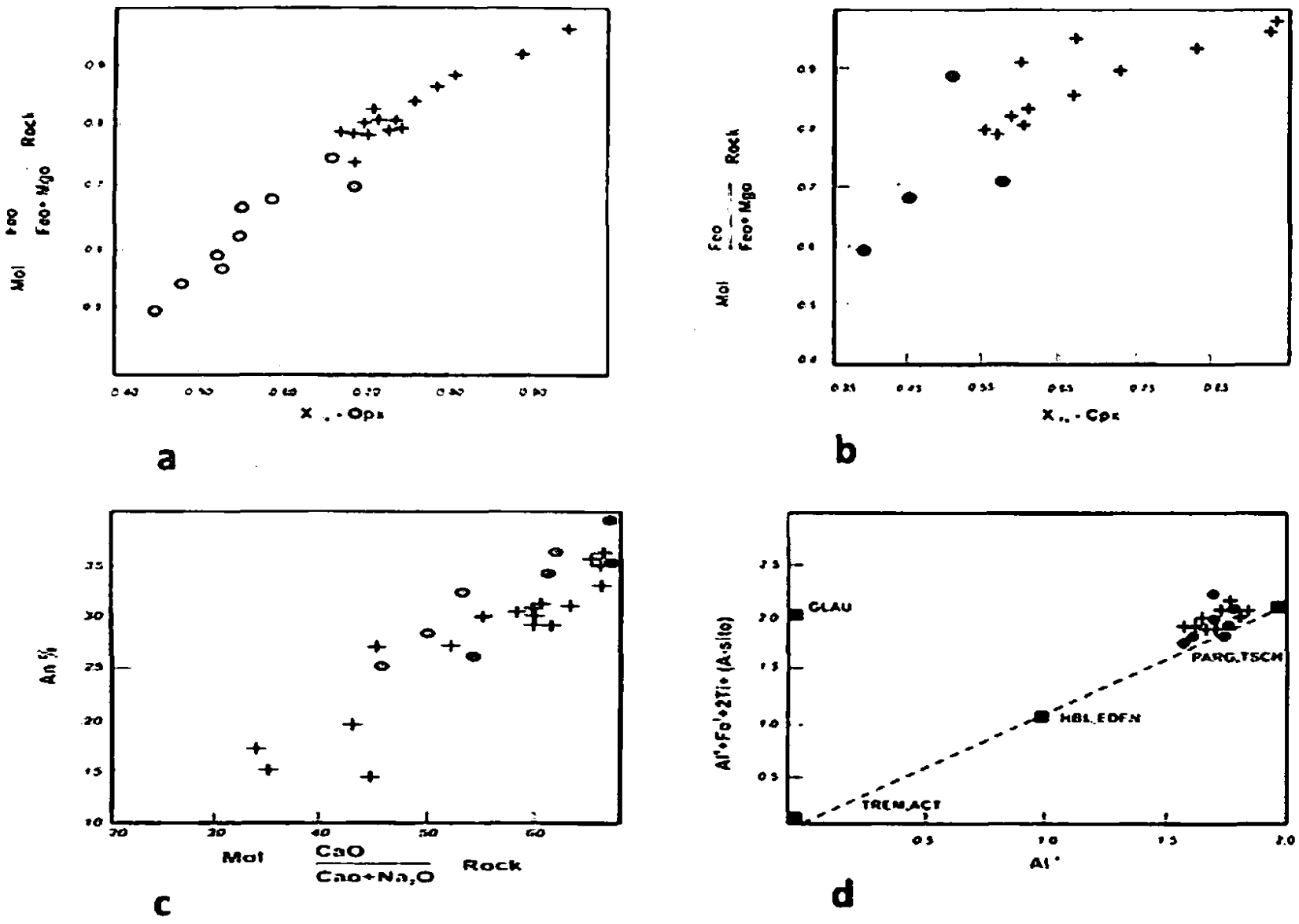

Fig. 4 (a) Dependence of X_{Fe} – Opx on bulk FeO/FeO+MgO ratio (filled circles for tonalitie/trondhjemitie , crosses for granitic rocks), (b) Variation between X_{Fe}-Cpx and bulk FeO/FeO+MgO ratio, (c) Variation of An content of plagioclase with CaO/CaO+Na_2O of host rock and (d) Composition of hornblende from granitic and tonalitic rocks (symbols as for Fig. 4a)

which is between 14% and 44% with X_{Ca} – rock is illustrated in Figure 4c.

AMPHIBOLES

Amphiboles were present in 23 rock samples (composition of amphibole formed along the edges of pyroxene are excluded). The structural formulae of apparently pre- or synkinematic amphibole analyses were calculated on13-cation (excl. Ca, K, Na) basis (Appendix Table 6). According to the nomenclature of Leake (1978) all amphiboles belong to the calcic group, irrespective of calculation method.

Fe^{+2}/Fe^{+3} ratios were calculated from the electron microprobe analyses after normalizing to 13-cations (excl. Ca, Na, K). Granitic samples generally have a higher Fe^{+2}/Fe^{+3} ratios (4-12) when compared with these ratios of tonalitic samples (0.4-4). The compositions of studied amphiboles are shown in relation to various end-members (Figure 4d). The positive correlation is due to exchange of edenite and tschermakite components but the deviation from end-member tie-line indicates substitution by Fe^{+3}, Ti^{+4} etc.

BIOTITE

Biotite was present only in 10 samples. Clearly, some of them contain secondary biotite while

others exhibit ambiguous textural relationships. X_{Fe} ranges from 0.42 to 0.93. Titanium contents are generally high, the highest being 0.70 p.f.u

WOLLASTONITE-SCAPOLITE-GARNET-GRANULITES AND ASSOCIATED ROCKS

The following section attempts to constrain the peak metamorphic temperatures of the granulite facies metamorphism of the study-area using equilibria of calc-silicate minerals, especially in the light of available internally consistent thermochemical data, improved activity-composition relations for grossular garnet and scapolite and well established paleopressure estimates (≥ 9kb) from garnet-pyroxene granulites.

PETROGRPAHY

As described elsewhere calc-silicate rocks mostly occur as lenses, boudins or minor intercalations with pyroxene granulites and impure marble. Samples U-143, R-163, R-206, AJ-1, and SAM-1are from the southeastern part of the HC near the Highaland-Vijayan boundary (Figure 1). It should also be noted that there are a number of granulite facies enclaves within this Vijayan area dominantly made up of amphibolite facies rocks.

Petrographic examination reveals the stable existence of following assemblages during peak metamorphism.

Scapolite + diopside + wollastonite + plagioclase + calcite + grossular ± quartz ± vesuvianite (AJ-1)

Scapolite + diopside + wolastonite + grossular + calcite + quartz (U-143)

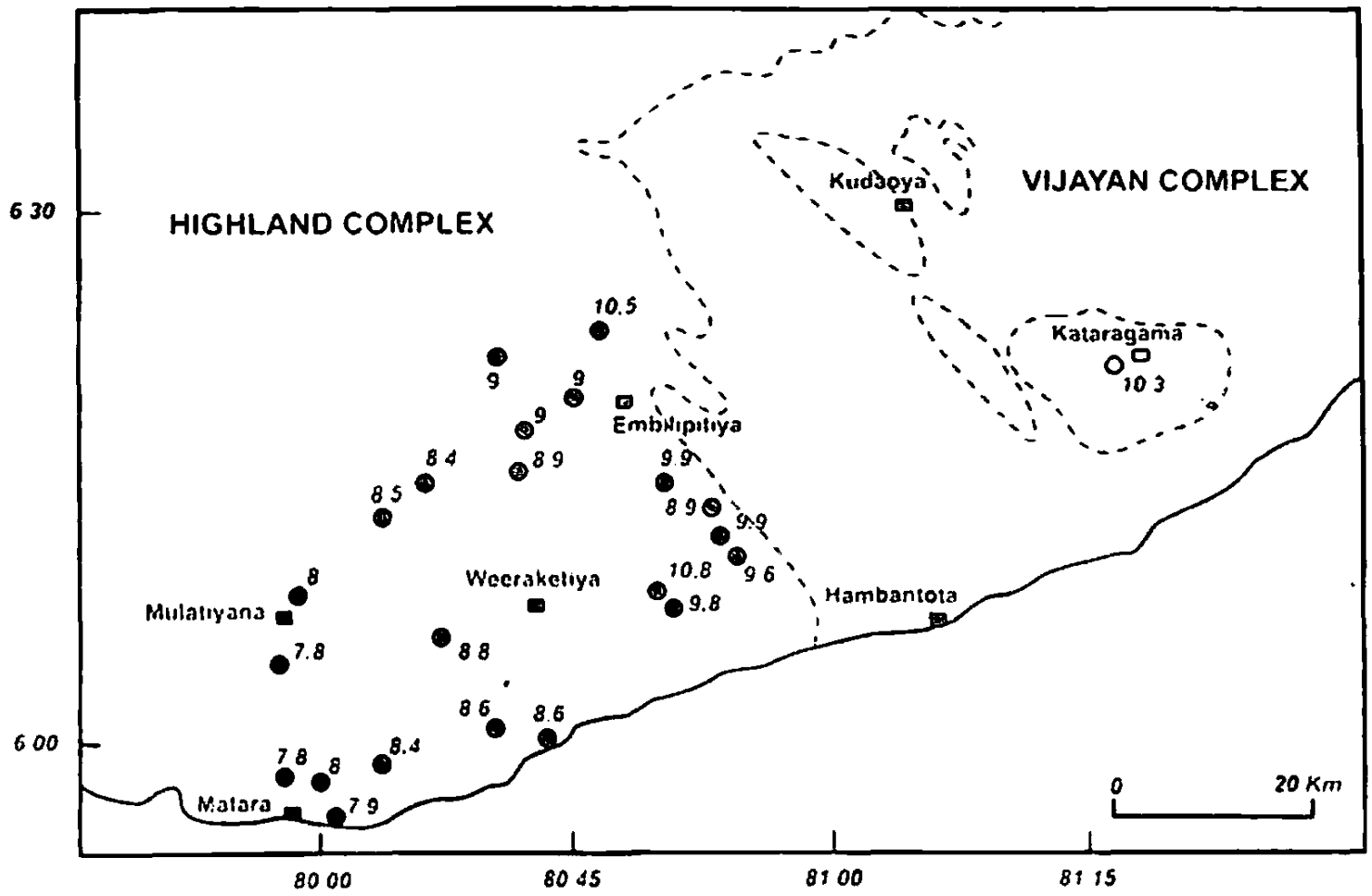

Fig. 5 Geographic variation of paleo-pressure estimates at 800°C according to Perkins and Chipera (1985). Note the pressure increase from about 7.5 kb from western part (i.e. Matara) to over 10 kb towards eastern part (i.e. HC/VC boundary).

Scapolite + diopside + plagioclase + grossular ± calcite ± quartz (R-163)

Scapolite + plagioclase + calcite + diopside± graphite (R-206)

Anorthite + garnet ± clinozoisite ± sphene ± magnetite (SAM-100)

Mineral constituents of the calc-silicate rocks are given in Appendix Table 9.

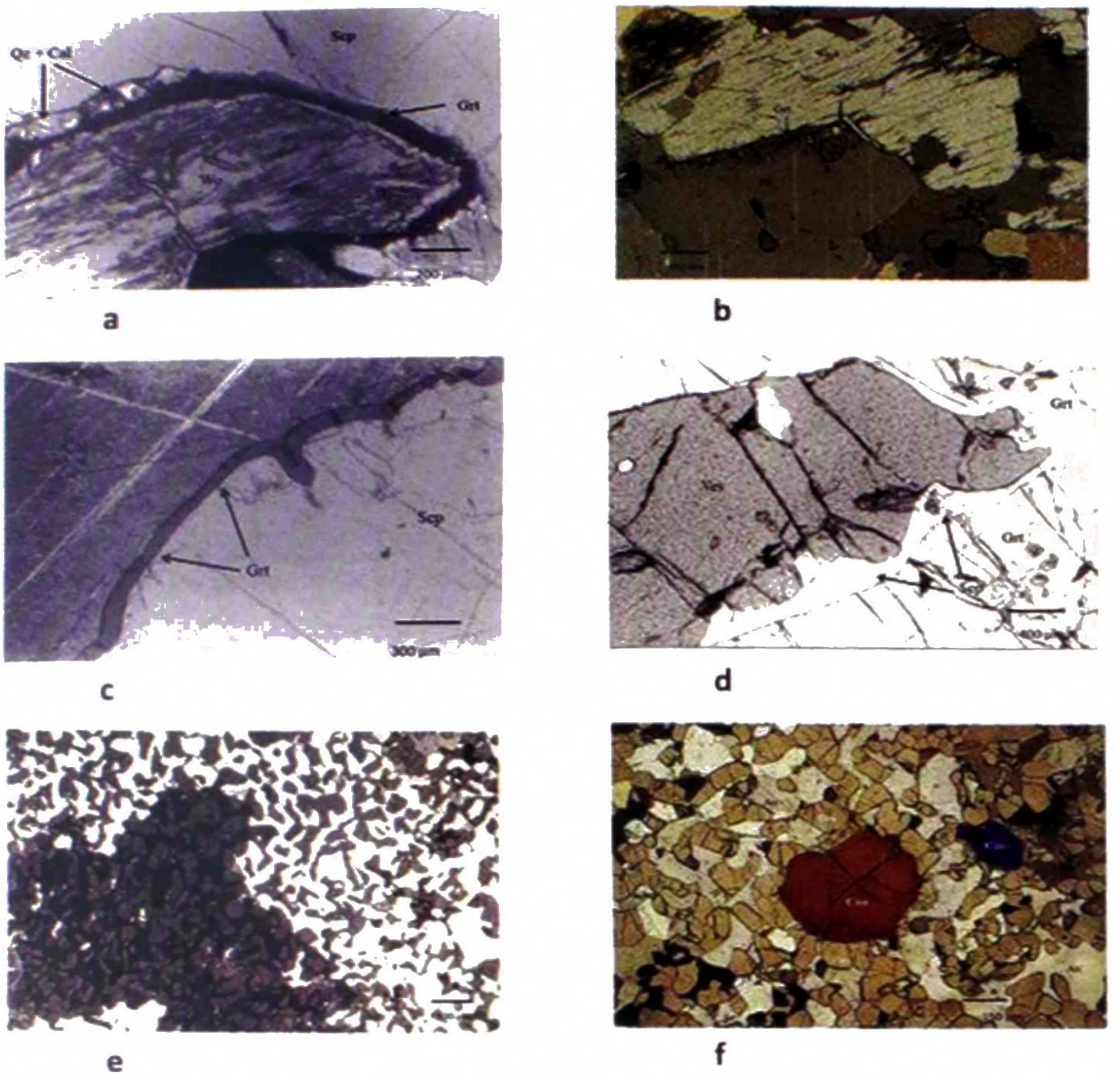

Fig. 6 (a) Garnet rim with quartz and calcite blebs formed between scapolite and wollastonite (U-143), (b) Garnet and quartz formed between plagioclase and wollastonite (AJ-1), (c) A garnet rim formed between scapolite and calcite, (d) Scapolite rims between vesuvianite and garnet (AJ-1), (e) Sieve garnet replacing anorthite with sporadic clinozoisite (SAM-100); note the large area in extinction probably showing a single grain of plagioclase now replaced by garnet (pseudomorph?) and (f) Clnozoisite-sieve garnet (Grs)-anorthite association in SAM-100.

Though there is no significant compositional difference between porphyroblastic garnet and coronal garnet textural evidence favours the formation of prograde as well as retrograde garnet. In contrast to the charnockitic pyroxene granulites, mineral assemblages in calc granulites vary within a given layer or an outcrop.

MINERAL REACTIONS

As in the case of many high-grade rocks there is no direct evidence for prograde reactions in these calc-silicate rocks. However, quartz and calcite inclusions in wollastonite (sample U-143,) are indicative of the reaction:

$$\text{calcite} + \text{quartz} \rightarrow \text{wollastonite} + CO_2 \quad \ldots\ldots\ldots (5)$$

RETROGRADE REACTIONS

Out of the retrograde mineral reactions, those leading to the formation of coronal garnet are most prominent. These garnet forming reactions are reported from many granulite grade terrains and interpreted as a consequence of near isobaric cooling of the lower crust after peak metamorphism. In sample U-143, garnet rims with calcite and quartz blebs occur between scapolite and wollastonite (Figure 6a). This observation can be explained by the fluid-absent reaction:

scapolite + 6 wollastonite →3 garnet + calcite + 3 quartz ---------- (6)

Presence of clinopyroxene (diopside) in the vicinity of some reaction domains may indicate the involvement of this mineral as a source of Fe for minor almandine component of the grossular garnet.

In sample AJ-1, thin garnet and quartz rims have been formed between wollastonite and plagioclase (Figure 6b). This textural relationship is consistent with the fluid-absent reaction:

2 wollastonite + plagioclase → garnet + quartz - ---------- (7)

vesuvianite (Figure 6d) and probably during a late metasomatic event.

Sample SAM-100 is from a silica undersaturated boudin near the Highland-Vijayan boundary. Its bulk composition is comparable to that of an anorthosite (SiO_2%=40, CaO%=26, $Al_2O_{3\%}$=23, FeO%=9). Over 90% this rock is made up of garnet and plagioclase. Garnet which appears to be replacing plagioclase is set in a matrix dominantly made of plagioclase, forming a sieve texture (Figure 6e). However, absence of quartz, wollastonite and scapolite makes it difficult to model garnet producing reaction that consumes plagioclase. Clinozoisite with straight contacts to garnet and plagioclase is present

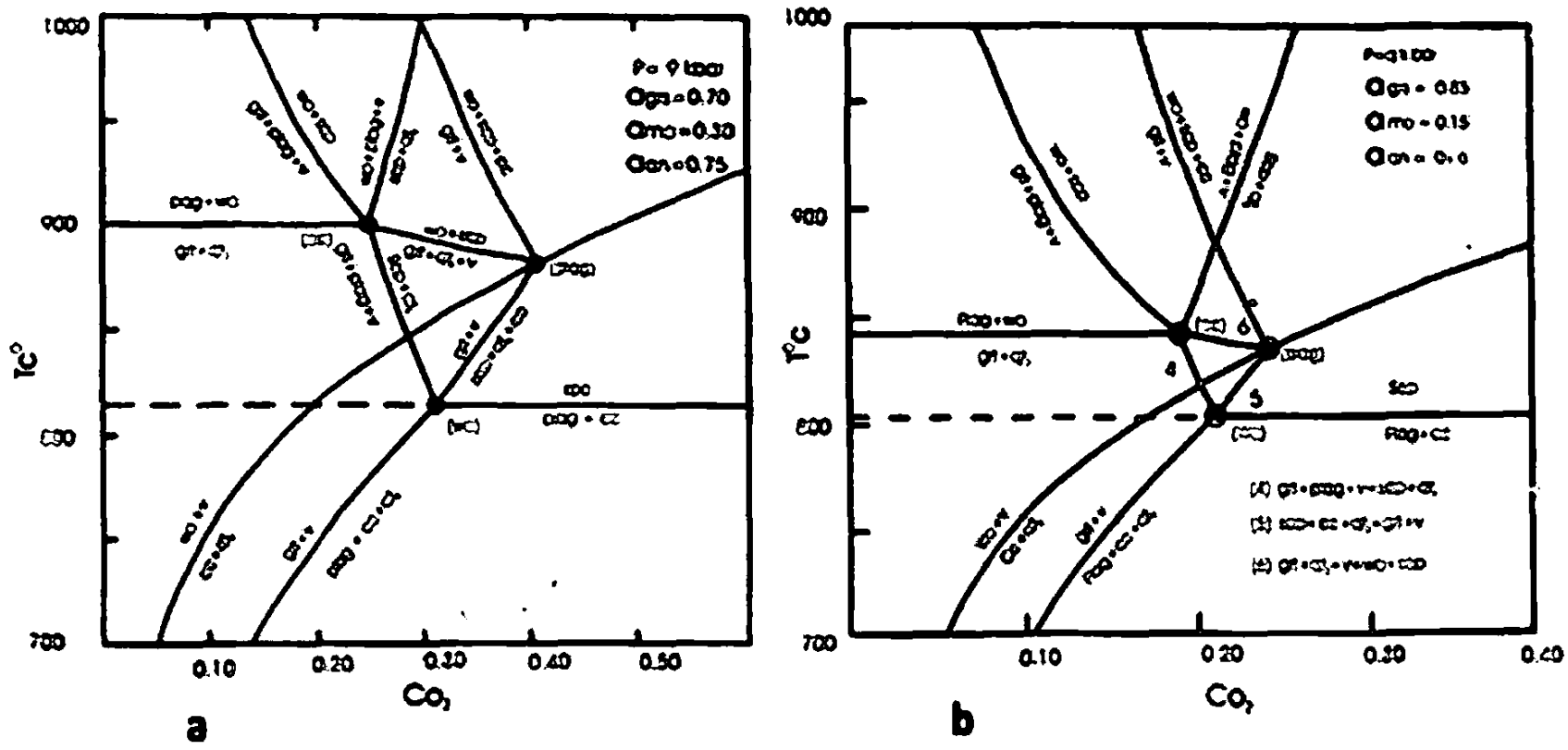

Fig. 7: T-$X_{(CO2}$ topology (a. sample R-163, b. sample AJ-1)

In sample U-143, garnet rims separating scapolite from calcite (Figure 6c) can be ascribed to the decarbonation reaction:

scapolite + 5 calcite + 3 quartz → 3 garnet + 6 CO_2 ---------- (8)

Other retrograde reactions indicative of subsequent cooling include rare cases of breakdown of wollastonite to form calcite + quartz (AJ-1) and decomposition of scapolite to plagioclase and calcite.

Other notable textural features observed include scapolite rims formed between garnet-

amounting to a model percentage of about 2%. There is no direct evidence to prove that this clinozoisite is a secondary product.

A calc-silicate rock with similar textural features has been reported from the Prince Olav Coast, East Antarctica (Hiroi et al., 1987). Subramaniam (1956) has also reported somewhat similar garnet-anorthite-clinozoisite rock from Sittampundi Complex, Madras State but mineral assemblage differs in having courundum.

MINERAL CHEMISTRY OF CALC SILICATE ROCKS

Representative microprobe analyses of scapolite + plagioclase and garnet + diopside from studied calc-granulite sample are given in Appendix Tables 10 and 11 respectively.

GARNET

Garnets are essentially grossular-andradite-almandine solid solutions with minor (usually <1%) pyrope and spessertine components. These compositions are similar to garnet compositions reported from calc silicate rocks of some other granulite terrains. Usually there is no compositional distinct between porphyroblastic garnet and coronal garnet but garnet rims between wollastonite and plagioclase (AJ-1) are highly calcic (X_{gr}=0.92). The highest andradite content is about 13% (SAM-100).

SCAPOLITE

Semi-quantitative microprobe analysis scapolite from all analyzed samples indicates that they are devoid of S and amount of Cl is very low except for AJ-1. They have AnEq (= [Al-3]/3 x 100 on the basis of Si+Al=12)) values between 55% and 78%. Scapolite compositions from sample AJ-1 vary significantly. Fresh-looking zones of scapolite are relatively low in Ca while dark and apparently altered zones are highly calcic. Variation of composition is apparently unrelated to any zoning pattern. A notable feature of the high-Ca analyses is unusual Si-Al substitution resulting in high Si/Al ratio and relatively low Me ([Al-3/3]) contents. Such compositional variations within a grain and unusual Si-Al substitution is possible as a result of crystallographic constraints imposed on two independent substitution schemes (e.g. Chamberlain et al., 1985; Hassan and Buseck, 1988; Sherriff et al., 2000).

PLAGIOCLASE

Although An content of the different samples varies greatly, there is no marked compositional variation within an individual sample or grain. Plagioclase from SAM-100 appears to be pure anorthite (Appendix Table 10).

PYROXENE

Clinopyroxenes are basically diopside-hedenbergite solid solutions with variable and minor amount of Al_2O_3 (Appendix Table 11). Mg/(Mg+Fe) ratio varies from 0.41 to 0.74.

T-X_{CO_2} RELATIONS IN WOLLASTONITE-SCAPOLITE-GARNET ROCKS

Electron microprobe analyses of minerals from calc-silicate rocks (Appendix Tables 10 and 11) and petrographic features indicate that garnet and diopside are low in Mg, Mn etc. and involvement of minerals such as sphene and ilmenite is also minimum. Therefore as a first approximation, mineral reactions in this rock can be modeled in CaO-Al_2O_3-SiO_2- Vapour system. In present study activity model of Engi and Wersin (1987) was adopted for grossular rich garnet. Calculation of meionite activity in scapolite is critical as different models available (Moecher et al., 1991; Baker and Newton, 1995) may significantly shift the invariant points and topology. Barker and Newton (1995) model which assumes complete disorder was adopted as peak temperatures would foreseeably exceed 750°C. Model proposed by Newton and Haselton (1982) was employed to calculate activity of anorthite. Analysis of scapolite for S and Cl from present calc-slicate rocks indicates that they are almost devoid of Cl and SO_4. Therefore in considering the fluid-mineral relations of these rocks our attention was focused on CO_2 and H_2O. As discussed in a succeeding chapter it is reasonable to assume that peak metamorphic pressure was not less than 9kb and garnet coronas were formed at an early stage of retrograde path. Therefore, T-X_{CO2} diagrams were constructed for samples R-163 (a_{Grs}=0.7, a_{Me}=0.3, a_{An}=0.75) and AJ-1 (a_{Gr}=0.85, a_{Me}=0.15, a_{An}=0.6), at 9kb using thermodynamic data set of Holland and Powell (1998) and PeRpLeX software by Conolly (1990). T-X_{CO2} topologies (Figures 7a and 7b) are similar to high-pressure (>9kb) pure CASV

topology of Warren et al. (1987) but An, Cal, and Wo invariant points for AJ-1 has slightly converged. The absence of wollastonite in R-163 Grt+Pl+Scp+Wo assemblage with given compositions would have buffered the X_{CO2} around 0.25 at a temperature not less than 875°C. For AJ-1, a T-X_{CO2} diagram was constructed using scapolite with highest Me content-An_{Eq}=62. Although T-X_{CO2} topology is similar to that of sample R-163, it has further shrinked and shifted towards lower temperatures. Co-existence of Grt+Wo+Pl+Scp again favours a minimum temperature of 850°C and XC_{O2} value of about 0.3. However, topology inverts when a_{Me} value is about 0.2 provided that other parameters remain unchanged. As mentioned earlier, there is unusual compositional variation in scapolite from AJ-1, probably as a result of crystallographic constraints imposed on substitution reactions. On such occasions, localized ordering of Al and Si can take place vitiating the validity of an activity model based on complete disorder.

Coexistence of plagioclase and wollastonite was observed only in above described samples (R-163, AJ-1). Lack of plagioclase in U-143 of which the mineral compositions are not much different may have been caused by higher X_{CO2} values (>0.3) in this sample. Different reactions involved in the formation of garnet coronas in AJ-1 and U-143 also indicate evolution of their retrograde path under different X_{CO2} conditions (Figures 7a and 7b). Cooling is essential to form garnet by solid-solid reactions 6 and 7 while appearance of garnet rims between calcite and scapolite may have been caused by lowering of CO_2 activity. In sample R-206 collected from the same area, calcite and quartz are in direct contact but there is no wollastonite. Lack of wollastonite in this sample which could also have been heated to a temperature not less than 850°C indicate high CO_2 activity. Presence of CO_2 bearing fluids is also indicated by intergranular graphite strings, specially between calcite and plagioclase.

Thus, calc-granulites and impure marble which were metamorphosed under more or less similar P-T conditions indicate significant differences in fluid conditions. Therefore it is reasonable to assume that the any fluids affected these calc-granultes were internally buffered by mineral equilibria in individual lithologies, if not even in local domains. In fact, heterogeneity of distribution of equilibrium assemblages suggests variation of fluid composition within a given lithology.

A more plausible explanation is that cooling of these rocks were caused by introduction of H_2O which also diluted CO_2 during retrogression.

THERMOMETRY BASED ON TEXTURAL RELATIONSHIPS OF CALC-SILICATE ROCKS

Clear textural relationships for the fluid-independent reactions (6) and (7) observed in sample U-143 and AJ-1 were used to obtain univariant reaction curves using activity corrected compositions and thermodynamic data set of Holland and Powell (1998). At 9 kb, reaction (6) in sample R-163 yields a minimum temperature of 850°C (Figure 8). Similarly, a minimum temperature of 825°C can be estimated for reaction (7) in sample AJ-1 (Figure 8).

PEAK METAMORPHIC CONDITIONS

From the present geobarometric study of the garnet-pyroxene granulites as well the previous studies it can be well established that the minimum palaeo pressures in the southeastern areas of the HC are 10±0.5 Kb (Tabl 8). These pressure estimates in conjunction with the various textural features and mineral compositions of the calc-silicate rocks can be used to ascertain the minimum peak metamorphic temperatures of the studied area.

Further, scapolite with high meonite from sample AJ-1 (Appendix Table 10) also wouldn't be stable at temperatures below 850°C. Thus it is evident that temperatures around or in excess of 875°C prevailed during peak metamorphism.

These temperatures are comparable with the highest temperatures obtained using Grt-Px cation exchange thermometry of charnockitic pyroxene granulites.. High temperature

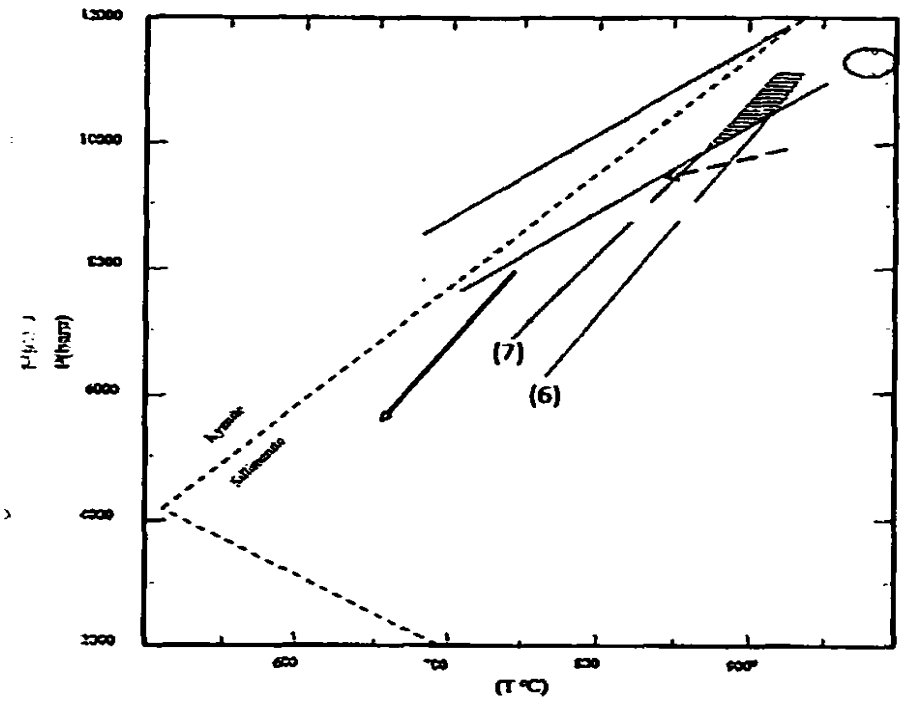

Fig. 8 Generalized P-T diagram illustrating possible peak metamorphic conditions (stippled oval), metamorphic conditions based on present study; probably representing a reset stage and postulated retrograde path. Stippled band shows the P-T spread given by seven (07) garnet-pyroxene-plagioclase-quartz samples from the southeastern Highland Complex near the Vijayan Complex boundary. Lines 6 and 7 are for the fluid independent reactions 6 and 7 observed in calc-silicate rocks from the same area.

assemblages indicating temperatures over 1000°C are reported from elsewhere in the HC by a number of studies (Osanai et al., 2006; Dharmapriya et al., 2013; Sajeev et al., 2007). Relatively low and scattered temperature estimates from the Grt-Px thermometry may be due to efficient but varying degrees of Fe^{+2}–Mg^{+2} re-equilibrium between garnet and pyroxene in different rock samples. Therefore it is reasonable to believe that temperatures yielded from calc-silicate equilibria are more representative of peak metamorphic temperatures. If this is the case, pressure estimates calculated at 800° C (Appendix Table 8) have to be incremented by about 01 kb in order to obtain a more realistic peak metamorphic pressure for the samples from the easternmost study-area.

P-T TRAJECTORY AND GEODYNAMIC IMPLICATIONS

Although rare kynite inclusions in garnet have been reported (e.g. Hiroi et al., 1994; Raase and Schenk, 1984) sillimanite inclusions are relatively abundant in pelitic rocks throughout the HC including the studied area.. This indicates that the prograde path within the kyanite stability filed was short-lived and much of it evolved within sillimanite stability field (Prame,1991). In fact, Raase et al. (1994) noticed a succession of sillimanite-kayanite-sillimanite inclusions distributed from core to rim. In Figure 8, stippled band shows the P-T spread given by seven (07) garnet-pyroxene-plagioclase-quartz samples from the southeastern HC near the VC boundary. Lines 6 and 7 are for the fluid independent reactions 6 and 7 observed in calc-silicate rocks from the same area. Formation of coronal garnet in calc-silicate rocks and some of the garnet pyroxene granulites can be attributed to near isobaric cooling as indicated by the arrow. Stabilization of iron-rich orthopyroxene (Fs_{95}; Appendix Table 3) instead of fayalite + quartz can also be explained by cooling under high pressure conditions. Previous studies carried out on garnet-pyroxene granulites from elsewhere in the HC have also reported textures supportive of near-isobaric cooling after peak metamorphism (Faulhaber and Raith, 1991; Schumacher et al., 1991; Prame, 1991). A previous study on a calc-silicate rock sample northeast of the study area has also given similar evidence (Mathavan and Fernando, 2001). Temperature estimates obtained using compositions of newly formed garnet and nearby clinopyroxene (Ellis and Green, 1978) are around 735°C. Even higher temperatures (750-800°C) would have prevailed during the formation of garnet as our calculated temperature is likely to represent a reset stage between Grt and Cpx.

Formation of orthopyroxene and plagioclase at the expense of garnet + quartz or grt+cpx+qtz in several samples (90-34 and 90-62) can be attributed to this decompression episode after near isobaric cooling. Caculations using

compositions of newly formed plagioclase, orthopyroxene and garnet rims indicate that this decompressional reaction took place at 6 Kb and 700°C.

Our paleo-pressure and -temperature estimates from south-easternmost HC (~10kb,'875) confirm burial of south-easternmost parts of the HC to deeper level (~ 40 km). Systematic decrease of pressure towards the west indicates that the study area represents a part of a tilted lower crustal block.

CONCLUSIONS

In the Southeastern HC of Sri Lanka, minor calc-silicate granulites occur in the form of lenses or boudins together with charnockitic rocks and quartzo-feldspathic gneisses. Garnet-orthopyroxene-plagioclase-quartz geobarometry of 25 charnockitic pyroxene granulite rocks from the south and southeastern Sri Lanka clearly displays a significant paleo-pressure increase towards the boundary between the Highland and Vijayan Complexes. Calculations at 800°C yields paleo-pressures around 10 kb in the southeastern HC, in full conformity with the results of the earlier studies. Wide range of temperature estimates obtained from garnet-pyroxene and two pyroxene thermometry represent varying reset stages. Estimations based on calc-silicate equilibria are suggestive of peak temperatures in excess of 875°C, at least in the southeastern areas of the HC near the HC-VC boundary. Therefore, paleo-pressure calculations for the samples from this area made at 800°C (Appendix Table 8) are to be incremented by about 01 Kb. Garnet-pyroxene granulites as well as minor calc-silicate rocks display mineral reactions indicative both near-isobaric cooling and decompression. Textural features observed in the present studies are compatible with an early stage of isobaric cooling prior and subsequent decompression. Further cooling at later stages of retrograde path is also indicated by breakdown of wollastonite to calcite and quartz, breakdown of scapolite to plagioclase and calcite and hydration reactions.

Mineral paragenesis and T-X_{CO2} diagrams imply that calc-silicate rocks from different localities had variable CO_2 activities between 0.2 and 0.5. However, one sample with graphite may indicate even higher X_{CO2} values. These results and heterogeneous distribution of assemblages in calc-silicate rocks are suggestive of internally buffered fluid phase.

Oxygen fugacity calculations for charnockitic pyroxene granulites also imply two different oxygen fugacity ranges, rocks of granitic-adamellitic composition having relatively low f_{O2} values compared to those of tonalitic-trondjhemitic composition. This could be the result of marked difference of bulk X_{Fe} values in these two rock types. However, variance of equilibrium assemblages within the granitic-ademellitic type or tonalitic-trondjhemitic type rocks is minimal. Such varying X_{CO2} values in calc granulites and contrasting f_{O2} values in different pyroxene granulites can be best explained by internal fluid buffering imposed by mineral phases and therefore these findings are at odds with a pervasive fluid infiltration hypothesis.

ACKNOWLEDGEMENTS

This paper is dedicated to the memory of Late Prof. Percival Gerald Cooray whose pioneering work on Sri Lankan Geology was a great inspiration to us. We thank two anonymous reviewers for their valuable comments. We are grateful to editors for their patience and understanding. Authors are indebted to Prof. Michael Raith (Bonn University), Dr. Beate Spiering (Bonn University) and Prof. Yoshikuni Hiroi (Chiba University) for facilitating microprobe analysis. The paper is published with the permission of the Director General, Geological Survey and Mines Bureau.

REFERENCES

Baker, J. -and Newton, R.C. (1995) Experimentally determined activity-composition relations for Ca-rich scapolite in the system $CaAl_2Si_2O_8$-$NaAlSi_3O_8$-$CaCO_3$ at 7 kbar. American Mineralogist, 80:744-751.

Berger, A.R. and Jayasinghe, N.R. (1976) Precambrian structures and geochronology in the Highland Series of Sri Lanka. Precambrian Research, 3:559-576.

Bhattacharya, A., Krishnakumar, K., Raith, M. and Sen, S.K. (1991). An improved set of a-X parameters in Fe-Mg-Ca garnets and refinement of the orthopyroxene-garnet thermometer and the garnet-orthopyroxene-plagioclase-quartz barometer. Journal of Petrology, 32:629-656.

Bhowmik, S.K., Dasgupta, S., Hoernes, S. and Bhattacharya, P.K. (1995) Extremely high-temperature calcareous granulites from the Eastern Ghats, india: Evidence for isobaric cooling, fluid buffering, and terminal channelized fluid flow. European Journal of Mineralogy, 7:689-703.

Bohlen, S.R. and Boettcher, A.L. (1981) Experimental investigations and geological applications of orthopyroxene geobarometry. American Mineralogist, 66:951-964.

Connolly, J.A.D. (1990) Multivariate pressure diagram: an algorithm based on generalized thermodynamics. American Journal of Science, 290:666-718.

Chamberlin, C.P., Docka, J.A., Post, J.E. and Burnham, C.W. (1985) Scapolite: Alkali atom configurations, antiphase domains, and compositional variations. American Mineralogist, 70:134-140.

Cooray, P.G. (1994) The Precambrian of Sri Lanka: A historical review. Precambrian Research, 66:3-18.

Dahl, P.S. (1980) The thermal-compositional dependence of Fe-Mg distributions between coexisting garnet and pyroxene: applications to geothermometry. American Mineralogist, 65:854-866.

Dharmapriya, P.L., S.P.K. Malaviarachchi, S.P.K., N.D. Subasinghe, N.D. and Dissanayake, C.B. (2013) Orthopyroxene-sillimanite-quartz assemblage in sapphirine granulites: Sign for ultra-high temperature metamorphism in the central HC, Sri Lanka. Proceedings to 29th Technical Sessions of Geological Society of Sri Lanka, 2013, 45-48

Ellis, D.J. and Green. D.H. (1979) An experimental study of the effect of Ca upon garnet-clinopyroxene Fe-Mg exchange equilibria. Contributions to Mineralogy and Petrology, 71:13-22.

Engi, M. and Wersin, P. (1987) Derivation and application of a solution model for calcic garnet. Schweizerische Mineralogische und Petrologische Mitteilungen, 67:53-73.

Faulhaber, S. and Raith, M. (1991) Geothermometry and geobarometry of high-grade rocks: A case study on garnet-pyroxene granulites in southern sri Lanka. Mineralogical Magazine, 55:33-56.

Frost, B. R. and Lindsley, D. H. (1992) Equilibria among Fe–Ti oxides, pyroxenes, olivine, and quartz: Part II. Application. American Mineralogist, 77:1004–1020.

Fitzsimons, I.C.W. and . Harley, S.L. (1994) Garnet-coronas in scapolite-wollastonite calc silicates from East Antarctica: the application and limitations of activity-corrected grids. Journal of Metamorphic Geology, 12:761-777.

Geological Map of Sri Lanka (1982) Geological Survey Department.

Geological Sheet No.20, Rakwana-Tangalla (2001) Geological Survey and Mines Bureau of Sri Lanka.

Geological Sheet No 21, Hambantota-Kataragama-Yala (2001) Geological Survey and Mines Bureau of Sri Lanka

Hapuarachchi, D.J.A.C. (1968) Cordierite and wollastonite bearing rocks of southwestern Ceylon. Geological Magazine, 105:317-324.

Harley, S., Fitzsimons, I.C.W. and Buick, I.S. (1994) Reactions and textures in wollastonite-scapolite granulites and their significance for pressure-temperature-fluid histories of high-grade terranes. Precambrian Research, 66:309-323.

Harley, S.L. and Buick, I.S. (1992) Wollastonite-scapolite asemblages as indicatoros of granulite pressure-temperature-fluid histories: The Rauer group, East Antarctica. Journal of Petrology, 33:693-728.

Harley, S.L. (1984) An experimental study of the partitioning of Fe and Mg between garnet and orthopyroxene. Contributions to Mineralogy and Petrology 86:359-373.

Hassan, I. and Buseck, P.R. (1998) HRTEM characterization of scapolite solid solutions. American Mineralogist, 73:119-134.

Hiroi, Y., Shiraishi, K., Motoyoshi, Y. and Katsushima, T. (1987) Progressive metamorphism of calc-silicate rocks from the Prince Olav and Soya Coasts, East Antarctica. Proceedings of the National Institute of Polar Research on Antarctica Geosciences, 1:73-97.

Hiroi, Y., Ogo, Y. and Namba, K. (1994) Evidence for prograde metamorphic evolution of Sri Lankan pelitic granulites, and implications for the development of continental crust. Precambrian Research 66, 245-263.

Hoffbauer, R., Hoernes, S. and Fioentini, E. (1994) Oxygen isotope thermometry based on a refined increment method and its application to granulite-grade rocks from Sri Lanka. Precambrian Research, 66:199-220.

Hoffbauer, R. and Spiering, B. (1994) Petrological phase equilibria and stable isotopic fractionations of carbonate-silicate parageneses from granulite-grade rocks of Sri Lanka. Precambrian Research, 66:325-349.

Holdaway, M.J. (1971) Stability of andalusite and aluminium silicate phase diagram. American Journal of Science, 272:97-131.

Holland, T.J.B. and Powell, R. (1998) An internally consistent thermodynamic data set for phases for of petrological interest. Journal of Metamorphic Geology, 16:309-343.

Hölzl, S., Köhler, H., Kröner, A., Jaeckel, P. and Liew, T.C. (1991) Geochronology of the Sri Lanka basement. In: Kröner, A. (ed.), The crystalline crust of Sri Lanka, Professional Paper 5, Geological Survey Department, Sri Lanka, pp 135-140.

Hormann P.K., Raith M., Raase P., Ackerman D., Seifert F. (1980) The granulite complex of Finnish Lapland: petrology and metamorphic conditions in the Ivalojoky-Inarijarvi area // Bull. Geol. Surv. Finland. Vol. 308. pp 100.

Kleinschrodt, R. (1994) Structural evolution at the eastern boundary of the Highland Complex (Sri Lanka). Precambrian Research, 66:39-57.

Kröner, A. Cooray, P.G. and Vitanage, P.W. (1991) Lithotectonic subdivision of the Precambrian Basement in Sri Lanka. The Crystalline Crust of Sri Lanka-Geological Survey Department of Sri Lanka, Professional Paper, 5:5-21.

Kröner, A., Williams, I.S., Compston, W., BAur, N., Vitanage, P.W. and Perera, L.R.K. (1987) Zircon ion microprobe dating of high-grade rocks in Sri Lanka. Journal of Geology, 95:775-791.

Leake, B.E. (1978) Nomenclature of amphiboles. American Mineralogist, 63:1023-1052.

Lindsley, D.H. and Frost, B.R. (1992). Equilibria among Fe-ti oxides, pyroxenes, olivine, and quartz: Part 1. Theory. American Mineralogist, 77:987-1003.

Lindsley, D.H. (1983) Pyroxene thermometry. American Mineralogist, 68:477-493.

Mathavan, V. and Fernando, G.W.A.R. (2001) Reaction textures in grossular-wollastonite-scapolite calc-silicate granulites from Maligawila, Sri Lanka: evidence for high-temperature isobaric cooling in the meta-sediments of the Highland Complex. Lithos, In press.

Milisenda, C.C. (1991) Compositional characteristics of the Vijayan Complex. In: Kröner, A. (ed.), The crystalline crust of Sri Lanka, Professional Paper 5, Geological Survey Department, Sri Lanka, pp 135-140.

Milisenda, C.C., Liew, T.C., Hofmann, A.W. and Kröner, A. (1988) Isotopic mapping of age provinces in Precambrian high-grade terrains: Sri Lanka. Journal of Geology, 96:608-615.

Moecher, D.P. and Essene, E.J. (1990) Phase equilibria for calcic scapolite, and implications of variable Al-Si disorder for P-T-, T-XCO2, and a-X relations. Journal of Petrology, 31:997-1024.

Newton, R.C. and Haselton, H.T. (1981) Thermodynamics of the garnet-plagioclase-Al_2SiO_5-quartz geobarometer. In: Newton, R.C., Navrotsky, A., Wood, B.J. (eds.), Thermodynamics of minerals and melts, Springer Verlag, Berlin, pp. 131-147.

Newton, R.C. and Perkins, D. (1982) Thermodynamic calibration of geobarometers based on the assemblages garnet-plagioclase-orthopyroxene-(clinopyroxene)-quartz. American Mineralogist, 67:203-222.

Newton, R.C. (1983) Geobarometry of high-grade rocks. American Journal of Science, 283A:1-28.

Ollila, P.W., Jaffe, H.W. and Jaffe, E.B. (1988) Pyroxene exsolution: An indicator of high-pressure igneous crystallization of pyroxene-bearing quartz syenite gneiss from the High Peaks region of the Adirondack Mountain. American Mineralogist, 73: 261-273.

Osanai, Y.,Sajeev, K., Owada, M., Kehelpannala, K.V.W., Prame, W.K.B.N., Nakano, N., Jayatilake, S. (2006) Metamorphic evolution of high-pressure and ultrahigh-temperature granulites from the Highland Complex, Sri Lanka, 28:20-37.

Perkins, D. and Chipera, S.J. (1985). Garnet-orthopyroxene-plagioclase-quartz barometry: refinement and application to the English River subprovince and the Minnesota River Valley. Contributions to Mineralogy and Petrology 89, 69-80.

Pouchou, J.L. and Pichoir, F. (1984) A new model for quantitative X-ray-microanalysis. Part 1: Application to the analysis of homogene samples. La Researche Aerospatile 3, 220-224.

Prame, W.K.B.N. (1991) Metamorphism and nature of the granulite-facies crust in southwestern Sri Lanka: Characterization by pelitic/psammopelitic rocks and associated granulites. In: Kröner, A. (ed.), The crystalline crust of Sri Lanka, Professional paper 5, Geological Survey Department, Sri Lanka, pp 188-197.

Prame, W.K.B.N. (1991) Petrology of the Kataragama Complex, Sri Lanka: Evidence for high P,T granulite facies metamorphism and subsequent isobaric cooling: In: Kröner, A. (ed.) The crystalline crust of Sri Lanka, Professional paper 5, Geological Survey Department, Sri Lanka, pp 200-224.

Prame, W.K.B.N. (1997) Geochemistry and Genesis of granitoid rocks from southern Sri Lanka. Mineralogy and Petrology, 60:245-265.

Raase, P. and Schenk, V. (1994) Phase relations in metapelites of the Highland Complex, Sri Lanka: Indications for a metamorphic zonation. Precambrian Research, 66:265-294.

Raheim, A. and Green, D.H. (1974). Experimental determination of the temperature and pressure dependence of the Fe-Mg partition coefficient for coexisting garnet and clinopyroxene. Contributions to Mineralogy,48:179-203.

Raith, M., Raase, P., Ackermand, D. and Lal, R.K. (1983) Regional geothermobarometry in the granulite facies terrane of South India, Transactions of Royal Society of Edinburgh (earth science), 73:221-244.

Robinson, P. (1982) The composition space of terrestrial pyroxenes-internal and external limits. Reviews in Mineralogy, 7:419-494.

Roisnson, P., Jaffe, H.W., Ross, M. and Klein, Jr.C. (1971) Orientation of exsolution lamellae in clinopyroxene and clinoamphiboles: consideration of optimal phase boundaries. American Mineralogist. 56:909-939.

Sajeev, K., Osanai, Y., Connolly, J.A.D. Suzuki, S., Ishioka, J., Kagami, H. and Rino.S. (2007) Extreme crustal metamorphism during a neoproterozoic event in Sri Lanka: A study of dry mafic granulites. Journal of Geology, 115:563-582.

Schenk, V. (1984) Petrology of Felsic Granulites, Metapelites, Metabasics, Ultramafics, and Metacarbonates from Southern Calabria (Italy): Prograde Metamorphism, Uplift and Cooling of a Former Lower Crust. Journal of Petrology, 25:255-298.

Schumacher, R. and Faulhaber, S. (1994) Summary and discussion of P-T estimates from garnet-plagioclase-quartz-bearing granulllite facies rocks from Sri Lanka. Precambrian Research, 66:295-308.

Schumacher, R., Schenk, V., Raase, P. and Vitanage, P. (1990) Granulite facies metamorphism of metabasic and intermediate rokcs in the Highland Series of Sri Lanka. In: Ashworth, J.R. and Brown, M. (eds.), High-grade metamorphism and crustal anatexis, Allen and Unwin, London, pp 235-271

Sen, S.K. and Bhattacharya, A. (1984) An orthopyroxene-garnet thermometer and its application to Madras charnockites. Contributions to Mineralogy and Petrology, 88:64-71.

Sen, S.K., Bhattacharya, S. and Acharaya, A. (1995). A multi-stage pressure-temperature record in the Chilka Lake granulites: the epitome of the metamorphic evolution of Eastern Ghats, India?. Journal of Metamorphic Geology, 13:287-298.

Sengupta, P., Sanyal. S., Dasgupta, S., Fukuoka, M., Eh, J. and Pal, S. (1997) Controls of mineral reactions in high-grade garnet-wollastonite-scapolite-bearing calcsilicate rocks: an example from Anakapalle, Eastern Ghats, India. Journal of Metamorphic Geology, 15:551-564.

Shaw, R.K. and Arima, M. (1996) High-temperature metamorphic imprint on calc-silicate granulites of Rayagada, Eastern Ghats, India: implication for the isobaric cooling path. Contributions to Mineralogy and Petrology, 126:169-180.

Sherriff, B.L., Sokolova E.V., Kabalov, Y.K., Jenkins, D.M., Kunath-Fandrei, G., Goetz, S., Jäger, C and Schneider J. (2000) Meonite: Rietveld structure-refinement, 29Si MAS and 27Al SATR NMR spectroscopy, and comments on the marialite-meionite series. The Canadian Mineralogist, 38: 1201-1213.

Subramaniam, A.P. (1956) Mineralogy and Petrology of the Sittampundi Complex, Salem District, Madras State, India. Bulletin of the Geological Society of America, 67:317-390.

Tracy, R.J. (1982) Compositional zoning and inclusions in metamorphic minerals. Reviews in Mineralogy, 10:355-393.

Voll. G. and Kleinschrodt, R. (1991) Sri Lanka: Structural, magmatic and metamorphic development of a Gondwana fragment. The Crystalline Crust of Sri Lanka-Geological Survey Department of Sri Lanka, Professional Paper 5, 22-51.

Warren, R.G., Hensen, B.J. and Ryburn, R.J. (1987) Wollastonite and scapolite in Precambrian calc-silicate granulites from Australia and Antarctica. Journal of Metamorphic Geology, 5:213-223.

Wells, P.R.A. (1977) Pyroxene thermometry in simple and complex systems. Contributions to Mineralogy and Petrology, 62:129-139.

Whitney, D.L. and Evans, B.W. (2010) Abbreviations for names of rock-forming minerals. American Mineralogist, 95:185-187.

Wones, D.R. (1989) Significance of the assemblage titanite+magnetite+quartz in granitic rocks. American Mineralogist, 74:744-749.

Wood, B.J. and Banno, S. (1973) Garnet-orthopyroxene and orthopyroxene-clinopyroxene relationships in simple and complex systems. Contributions to Mineralogy and Petrology, 42:109-124.

APPENDIX

Appendix Table 1 Mineral constituents present in charnockitic granulite samples and their compositional/other notable features.

Samples	Grt	Opx	Cpx	Pl	Kfs	Amp	Bt	Qz	Composition/Notable Features
90-73	+	-	+	+	+	+		+	adamellitic comp.
91-15		-	+	+	+	-	-	+	adamellitic comp. Kfs in the form of Mc
91-14	+	-	+	-	+	+	+	+	adamellitic comp. Kfs in the form of Mc
90-76	-	+	-	+	+	+	+	+	dioritic comp. Kfs is rare
90-69	-	+	-	+	+	+	+	+	trondjhemitic comp. Kfs is rare
B-119	-	+	-	+	+	+	+	+	tonalitic comp. altered Opx
90-59	-	+	-	+	+	-	+	+	granodioritic comp.
90-77	+	+	+	+	+	+	-	+	monzonite comp.
B-117	+	+	+	+	+	+	-	+	adamellitic comp. coronal garnet
B-25	+	-	+	+	+	+	-	+	granitic comp. coronal garnet. secondary Opx
90-43	+	+	+	+	+	+	+	+	adamellitic comp. Cpx as inclusions in Opx
90-47	+	+	+	+	+	-	+	+	dioritic comp.
91-20	+	+	+	+	+	-	+	+	tonalitic comp. Cpx as inclusions in Grt
B-109	+	+	-	+	+	+	-	+	adamellitic comp.
B-108	+	+	-	+	+	+	-	+	adamellitic comp.
90-70	+	+	-	+	+	+	+	+	tonalitic comp.
9049	+	+	-	+	+	+	-	+	tondhjermitic comp. Kfs is rare
90-41	-	+	+	+	+	+	-	+	tonalitic comp.
90-52	+	+	-	+	+	+	+	+	tonalitic comp.
90-68	-	+	-	+	-	+	-	+	tonalitic comp. Kfs is rare
90-57	+	+	-	+	+	+	-	+	adamellitic comp.
90-46	+	+	-	+	+	+	+	+	granitic comp. Kfs in the form of Mc
90-54	+	+	+	+	+	-	-	+	dioritic omp?
90-34	+	+	+	+	+	+	-	+	adamellitic comp.
90-56	+	+	+	+	+	+	-	+	monzonitic comp.
90-66	+	+	+	+	+	-	-	+	monzonitic comp. Cpx as inclusions in Opx
90-30	+	+	+	+	+	-	-	+	monzonitic comp.
90-29	+	+	-	+	+	+	-	+	adamellitic comp.
90-61	+	+	+	+	+	+	-	+	adamellitic comp.
90-58	+	+	-	+	+	+	-	+	adamellitic comp.
90-62	+	+	+	+	+	+	-	+	granitic comp.
90-48	+	+	-	+	+	-	-	+	trondhjemitic comp.
90-36	+	+	-	+	+	+	-	+	adamellitic comp.
90-71	-	+	-	+	+	+	-	+	tonalitic comp.

Appendix Table 2a Representative electron-microprobe analysis of garnet cores of charnockitic granulites.

Samples	90-66	90-61	90-30	90-29	90-58	90-62	90-48	90-36	90-56	90-34	90-54	90-46	90-52	90-52
Na_2O (wt %)	0.00	0.02	0.00	0.02	0.00	0.01	0.01	0.02	0.01	0.00	0.01	0.00	0.00	0.01
K_2O	0.00	0.01	0.00	0.00	0.00	0.00	0.00	0.00	0.00	0.00	0.00	0.00	0.00	0.01
CaO	7.12	6.82	6.81	6.99	6.58	7.16	5.92	7.37	7.16	7.09	7.10	6.74	8.86	6.33
MgO	0.67	1.85	2.09	1.87	2.21	1.47	2.67	1.96	2.58	1.94	4.49	1.19	5.80	2.63
MnO	2.37	0.86	1.00	1.09	1.16	0.66	0.75	1.16	0.88	0.99	0.92	2.78	2.23	0.84
FeO	32.31	33.29	31.73	31.72	31.40	33.02	32.21	31.77	31.12	31.40	28.61	31.15	23.91	32.03
Cr_2O_3	0.00	0.00	0.04	0.03	0.00	0.00	0.05	0.04	0.00	0.04	0.05	0.00	0.00	0.04
Al_2O_3	19.93	20.89	20.50	20.30	20.64	20.33	20.79	20.39	20.54	19.95	20.87	19.78	21.09	20.63
TiO_2	0.07	0.09	0.12	0.08	0.04	0.11	0.05	0.09	0.09	0.10	0.15	0.04	0.05	0.08
SiO_2	36.68	36.67	37.01	36.93	37.32	36.59	36.93	37.30	37.04	37.13	37.84	36.70	38.03	36.93
Total	99.84	100.50	99.29	99.07	99.35	99.36	99.38	100.09	99.44	99.21	100.05	99.32	99.97	99.52
Na	0.000	0.006	0.000	0.005	0.000	0.004	0.004	0.005	0.005	0.000	0.004	0.000	0.001	0.004
K	0.000	0.002	0.000	0.000	0.000	0.000	0.000	0.000	0.000	0.000	0.001	0.000	0.000	0.001
Ca	1.245	1.177	1.181	1.217	1.138	1.249	1.024	1.270	1.237	1.232	1.201	1.180	1.484	1.095
Mg	0.164	0.443	0.504	0.454	0.531	0.357	0.643	0.471	0.620	0.469	1.08	0.290	1.351	0.632
Mn	0.328	0.117	0.137	0.150	0.159	0.091	0.103	0.158	0.121	0.136	0.123	0.384	0.295	0.115
Fe^{+2}	4.407	4.482	4.294	4.310	4.235	4.497	4.349	4.272	4.196	4.258	3.780	4.256	3.127	4.323
Fe^{+3}	0.083	0.000	0.000	0.004	0.000	0.000	0.000	0.000	0.000	0.069	0.000	0.115	0.000	0.000
Cr	0.000	0.000	0.005	0.004	0.000	0.000	0.006	0.005	0.000	0.005	0.007	0.000	0.000	0.005
Al	3.830	3.963	3.910	3.887	3.925	3.902	3.956	3.864	3.903	3.814	3.886	3.809	3.887	3.924
Ti	0.009	0.011	0.015	0.010	0.005	0.014	0.006	0.11	0.11	0.012	0.018	0.005	0.006	0.010
Si	5.983	5.904	5.990	6.001	6.019	5.959	5.962	6.000	5.972	6.023	5.979	5.996	5.948	5.960
a_{Grs}	0.178	0.188	0.191	0.196	0.189	0.199	0.167	0.204	0.201	0.181	0.199	0.162	0.254	0.177

Journal of Geological Society of Sri Lanka Vol. 16 (2014), 170-205
Professor P.G. Cooray Memorial Volume

Appendix Table 2b Representative electron-microprobe analysis of garnet cores of charnockitic granulites.

Samples	90-47	91-20	90-49	B-108	B-109	91-14	90-43	90-77	90-70	91-73	B-25
Na_2O (wt %)	0.00	0.00	0.00	0.02	0.00	0.01	0.01	0.02	0.00	0.00	0.03
K_2O	0.02	0.00	0.00	0.02	0.01	0.00	0.00	0.01	0.01	0.04	0.03
CaO	7.22	7.07	6.46	7.08	7.01	8.60	6.67	6.82	7.04	7.72	7.71
MgO	3.75	4.31	3.55	2.01	2.09	0.11	2.34	2.35	5.59	1.26	0.21
MnO	1.17	2.44	2.33	1.15	0.90	4.72	0.98	0.75	2.30	0.63	1.55
FeO	28.75	26.89	28.96	31.91	31.46	28.45	32.11	32.09	24.91	32.78	32.98
Cr_2O_3	0.00	0.01	0.00	0.00	0.00	0.03	0.02	0.00	0.02	0.03	0.00
Al_2O_3	20.61	21.38	20.02	20.05	20.04	19.73	20.60	20.84	20.44	20.41	20.24
TiO_2	0.06	0.04	0.04	0.08	0.03	0.04	0.07	0.11	0.06	0.08	0.01
SiO_2	37.77	38.01	37.34	37.17	37.73	36.62	37.01	37.36	37.92	36.88	36.45
Total	99.35	100.16	99.26	99.96	99.82	99.30	99.80	100.34	98.69	99.83	99.44
Na (atoms)	0.001	0.000	0.000	0.008	0.000	0.003	0.005	0.005	0.000	0.005	0.010
K	0.004	0.000	0.000	0.004	0.003	0.000	0.000	0.002	0.002	0.008	0.006
Ca	1.235	1.193	1.114	1.224	1.208	1.509	1.152	1.170	1.266	1.341	1.353
Mg	0.891	1.012	0.851	0.483	0.500	0.027	0.562	0.559	1.324	0.305	0.050
Mn	0.158	0.326	0.317	0.157	0.123	0.655	0.134	0.102	0.310	0.086	0.215
Fe^{+2}	3.836	3.539	3.896	4.306	4.230	3.897	4.329	4.293	3.307	4.441	4.519
Fe^{+3}	0.000	0.000	0.065	0.059	0.066	0.122	0.000	0.000	0.000	0.000	0.028
Cr	0.000	0.002	0.004	0.000	0.000	0.004	0.002	0.000	0.003	0.004	0.000
Al	3.875	3.966	3.796	3.812	3.797	3.808	3.913	3.928	3.824	3.897	3.908
Ti	0.007	0.005	0.005	0.009	0.004	0.005	0.008	0.013	0.007	0.009	0.001
Si	6.025	5.983	6.008	5.998	6.066	5.999	5.965	5.976	6.019	5.975	5.972
a_{Grs}	0.207	0.204	0.166	0.182	0.182		0.187	0.191	0.217		0.221

Appendix Table 3a Representative electron-microprobe analysis of interior of orthopyroxene of charnockitic granulites.

Samples	90-66	90-61	90-30	90-29	90-58	90-62	90-48	90-36	90-56	90-34	90-54	90-46	90-52	90-57	90-47
Na_2O (wt)	0.00	0.01	0.02	0.00	0.00	0.00	0.01	0.02	0.00	0.00	0.01	0.00	0.01	0.00	0.00
K_2O	0.01	0.00	0.00	0.01	0.01	0.00	0.00	0.02	0.02	0.00	0.00	0.00	0.00	0.01	0.00
CaO	1.05	0.90	0.95	0.93	0.76	0.98	0.68	0.68	0.86	1.12	0.79	0.67	0.60	0.81	0.85
MgO	3.24	7.43	8.98	7.82	9.88	5.57	10.86	8.33	9.79	8.19	14.96	6.34	18.32	10.36	13.58
MnO	1.24	0.43	0.41	0.56	0.48	0.32	0.34	0.48	0.46	0.52	0.41	1.26	1.03	0.37	0.64
FeO	47.73	43.29	40.29	41.62	39.19	45.04	38.67	42.05	39.15	41.27	32.43	43.47	26.51	38.73	34.56
Cr_2O_3	0.00	0.03	0.07	0.00	0.03	0.04	0.01	0.00	0.00	0.00	0.00	0.02	0.02	0.04	0.42
Al_2O_3	0.20	0.46	0.49	0.53	0.52	0.40	0.73	0.33	0.53	0.47	0.84	0.31	1.16	0.50	0.42
TiO_2	0.08	0.14	0.08	0.10	0.06	0.13	0.09	0.12	0.13	0.08	0.12	0.11	0.06	0.10	0.08
SiO_2	46.06	46.97	47.83	47.45	48.42	46.92	48.06	47.69	48.09	47.62	50.36	46.96	50.58	48.17	49.84
Total	99.62	99.67	99.13	99.01	99.35	99.41	99.44	99.72	99.03	99.25	99.91	99.14	98.30	99.10	100.01
Na (atoms)	0.000	0.001	0.002	0.000	0.000	0.000	0.001	0.002	0.000	0.000	0.001	0.000	0.000	0.000	0.000
K	0.001	0.000	0.000	0.000	0.001	0.000	0.000	0.001	0.001	0.000	0.000	0.000	0.000	0.001	0.000
Ca	0.048	0.040	0.042	0.041	0.033	0.044	0.030	0.030	0.038	0.050	0.033	0.030	0.025	0.036	0.036
Mg	0.208	0.463	0.553	0.486	0.603	0.351	0.660	0.514	0.600	0.507	0.874	0.399	1.062	0.633	0.804
Mn	0.045	0.015	0.014	0.020	0.017	0.012	0.012	0.017	0.016	0.018	0.014	0.045	0.034	0.013	0.022
Fe^{+2}	1.712	1.499	1.375	1.439	1.333	1.582	1.289	1.446	1.333	1.414	1.058	1.526	0.851	1.310	1.147
Fe^{+3}	0.005	0.014	0.017	0.012	0.008	0.008	0.030	0.011	0.013	0.018	0.005	0.008	0.011	0.017	0.000
Cr	0.000	0.001	0.002	0.000	0.001	0.001	0.001	0.000	0.001	0.000	0.000	0.001	0.001	0.001	0.020
Al	0.010	0.023	0.024	0.026	0.025	0.020	0.035	0.016	0.025	0.023	0.039	0.015	0.053	0.024	0.003
Ti	0.03	0.005	0.003	0.003	0.002	0.004	0.003	0.004	0.004	0.002	0.003	0.003	0.002	0.003	0.003
Si	1.981	1.962	1.976	1.978	1.981	1.981	1.960	1.975	1.977	1.977	1.975	1.981	1.966	1.974	1.978
a_{Fs}	0.897	0.786	0.744	0.772	0.704	0.832	0.703	0.764	0.724	0.763	0.605	0.809	0.518	0.712	0.634

Journal of Geological Society of Sri Lanka Vol. 16 (2014), 170-205
Professor P.G. Cooray Memorial Volume

Appendix Table 3b Representative electron-microprobe analysis of interior of orthopyroxene of charnockitic granulites.

Samples	91-20	90-49	B-108	B-109	90-43	90-77	90-70	90-41	90-76	90-68	B-117
Na_2O (wt	0.00	0.03	0.02	0.03	0.00	0.00	0.00	0.04	0.01	0.02	0.03
K_2O	0.00	0.00	0.00	0.01	0.00	0.00	0.00	0.00	0.01	0.00	0.01
CaO	0.88	0.75	0.94	0.70	0.80	0.91	0.69	0.85	0.69	0.81	0.81
MgO	15.82	14.45	7.96	9.04	9.38	9.35	17.26	9.73	17.66	14.41	1.24
MnO	1.00	0.79	0.50	0.31	0.40	0.33	1.80	0.65	0.69	1.24	0.64
FeO	31.32	33.18	41.89	40.55	41.29	40.82	28.59	39.27	29.70	32.73	50.47
Cr_2O_3	0.00	0.00	0.04	0.00	0.04	0.03	0.00	0.00	0.00	0.00	0.00
Al_2O_3	0.52	0.71	0.53	0.42	0.56	0.50	0.75	0.32	0.93	0.75	0.32
TiO_2	0.06	0.09	0.11	0.10	0.12	0.09	0.01	0.16	0.12	0.06	0.11
SiO_2	50.74	49.65	47.81	48.82	47.48	47.99	50.44	48.31	50.65	49.43	45.98
Total	100.35	99.64	99.80	99.97	100.07	100.02	99.54	99.35	100.45	99.45	99.60
Na (atoms)	0.000	0.002	0.001	0.002	0.000	0.000	0.000	0.004	0.001	0.002	0.002
K	0.000	0.000	0.000	0.000	0.000	0.000	0.000	0.000	0.000	0.000	0.001
Ca	0.037	0.032	0.042	0.031	0.035	0.040	0.029	0.038	0.029	0.034	0.038
Mg	0.918	0.853	0.491	0.550	0.575	0.571	1.002	0.595	0.015	0.853	0.080
Mn	0.033	0.027	0.018	0.011	0.014	0.012	0.059	0.023	0.022	0.042	0.024
Fe^{+2}	1.000	1.069	1.434	1.385	1.402	1.382	0.897	1.338	0.958	1.087	1.833
Fe^{+3}	0.020	0.030	0.014	0.000	0.018	0.018	0.034	0.009	0.000	0.000	0.000
Cr	0.000	0.000	0.001	0.000	0.001	0.001	0.000	0.000	0.000	0.000	0.000
Al	0.024	0.033	0.026	0.020	0.027	0.024	0.035	0.016	0.042	0.035	0.016
Ti	0.002	0.003	0.003	0.003	0.004	0.003	0.000	0.005	0.003	0.002	0.003
Si	1.976	1.967	1.977	1.993	1.953	1.967	1.964	1.981	1.953	1.963	1.997
a_{Fs}	0.589	0.617	0.770	0.744	0.741	0.739	0.548	0.548			0.959

Appendix Table 4 Representative electron-microprobe analysis of interior of clinopyroxene of charnockitic granulites..

Samples	91-15	91-14	90-77	90-43	91-20	90-47	90-41	90-54	90-34	90-56	90-66	90-61	90-30	90-62	B-117
Na_2O (wt%)	0.69	0.76	0.35	0.40	0.28	0.36	0.38	0.30	0.24	0.40	0.45	0.38	0.31	0.35	0.48
K_2O	0.01	0.02	0.02	0.01	0.00	0.00	0.00	0.00	0.00	0.00	0.00	0.01	0.01	0.02	0.01
CaO	20.21	19.83	21.10	20.91	22.46	20.33	20.93	21.95	20.96	21.54	20.89	20.18	19.27	20.67	19.11
MgO	5.58	0.77	7.60	8.11	11.93	10.71	7.75	11.37	7.17	8.00	3.02	6.10	7.31	4.76	1.18
MnO	1.75	1.73	0.23	0.16	0.44	0.33	0.27	0.12	0.19	0.21	0.55	0.18	0.24	0.22	0.37
FeO	20.55	27.92	18.87	19.23	12.75	16.27	18.89	12.05	19.75	17.83	25.89	21.58	21.01	23.25	29.05
Cr_2O_3	0.00	0.00	0.05	0.01	0.04	0.00	0.00	0.02	0.00	0.05	0.00	0.00	0.04	0.01	0.05
Al_2O_3	1.19	1.24	1.21	1.56	1.19	1.42	1.05	1.38	0.92	1.59	0.75	1.32	1.30	1.23	0.87
TiO_2	0.17	0.19	0.17	0.25	0.19	0.14	0.17	0.19	0.13	0.30	0.17	0.21	0.20	0.22	0.13
SiO_2	49.04	47.49	49.80	49.60	51.38	50.93	49.57	51.91	49.76	49.60	48.16	49.29	49.43	48.28	48.10
Total	99.19	99.95	99.40	100.22	100.66	100.49	99.01	99.30	99.13	99.53	99.88	99.25	99.12	99.00	99.35
K (atoms)	0.001	0.001	0.001	0.000	0.000	0.000	0.000	0.000	0.000	0.000	0.000	0.000	0.001	0.001	0.001
Ca	0.867	0.876	0.890	0.876	0.912	0.835	0.888	0.896	0.890	0.905	0.912	0.862	0.820	0.896	0.845
Mg	0.333	0.048	0.446	0.473	0.674	0.612	0.457	0.646	0.424	0.468	0.183	0.362	0.432	0.287	0.073
Mn	0.060	0.061	0.008	0.005	0.014	0.011	0.009	0.004	0.006	0.007	0.019	0.006	0.008	0.008	0.013
Fe^{+2}	0.689	0.899	0.586	0.564	0.342	0.471	0.577	0.384	0.631	0.536	0.852	0.694	0.673	0.738	0.989
Fe^{+3}	0.000	0.070	0.036	0.064	0.062	0.051	0.048	0.000	0.024	0.048	0.030	0.025	0.025	0.049	0.015
Cr	0.000	0.000	0.002	0.000	0.001	0.000	0.000	0.001	0.000	0.002	0.000	0.000	0.001	0.000	0.002
Al	0.056	0.060	0.056	0.072	0.053	0.064	0.049	0.062	0.043	0.073	0.036	0.062	0.061	0.059	0.042
Ti	0.005	0.006	0.005	0.008	0.005	0.004	0.005	0.005	0.004	0.009	0.005	0.006	0.006	0.007	0.004
Si	1.965	1.959	1.962	1.939	1.947	1.952	1.961	1.977	1.972	1.945	1.961	1.965	1.962	1.953	1.986

Journal of Geological Society of Sri Lanka Vol. 16 (2014), 170-205
Professor P.G. Cooray Memorial Volume

Appendix Table 5a Representative electron-micraprobe analysis of interior of plagioclase of charnockitic granulites.

Samples	91-20	90-49	B-108	B-109	91-14	90.-43	90-77	90-70	90-41	90.76	90-68	91-15	90-73	B-117
Na_2O (wt %)	7.27	8.16	7.93	8.32	10.09	8.21	8.07	7.58	8.50	7.26	7.41	9.29	7.93	10.45
K_2O	0.36	0.42	0.21	0.21	0.22	0.17	0.20	0.67	0.37	0.66	0.45	0.18	0.25	0.13
CaO	7.86	5.89	7.09	6.30	2.93	6.73	6.59	6.89	5.59	7.37	7.33	3.76	5.69	3.15
MgO	0.00	0.00	0.00	0.00	0.00	0.00	0.00	0.01	0.00	0.02	0.01	0.00	0.01	0.00
MnO	0.00	0.02	0.01	0.03	0.00	0.00	0.03	0.00	0.04	0.00	0.00	0.02	0.05	0.05
FeO	0.03	0.10	0.11	0.01	0.07	0.07	0.07	0.04	0.08	0.16	0.11	0.06	0.08	0.09
Cr_2O_3	0.00	0.01	0.00	0.04	0.00	0.00	0.00	0.05	0.05	0.00	0.02	0.06	0.01	0.00
Al_2O_3	26.08	24.43	25.69	24.54	22.00	25.49	25.11	24.74	23.77	25.56	25.27	22.76	24.31	21.00
TiO_2	0.00	0.00	0.00	0.01	0.01	0.06	0.01	0.01	0.00	0.02	0.01	0.02	0.01	0.03
SiO_2	59.56	60.61	58.93	60.55	65.24	60.33	60.56	59.75	61.80	59.50	59.11	64.68	62.73	65.95
Total	101.16	99.64	99.97	100.01	100.54	101.06	100.64	99.65	100.19	100.54	99.72	100.81	101.08	100.85
Na (atoms)	0.623	0.707	0.688	0.719	0.857	0.703	0.693	0.659	0.731	0.626	0.645	0.788	0.674	0.887
K	0.020	0.024	0.012	0.012	0.012	0.010	0.011	0.039	0.021	0.038	0.026	0.010	0.014	0.007
Ca	0.372	0.282	0.340	0.301	0.138	0.318	0.313	0.327	0.266	0.351	0.352	0.176	0.267	0.148
Mg	0.000	0.000	0.000	0.000	0.000	0.000	0.000	0.001	0.000	0.001	0.001	0.000	0.001	0.000
Mn	0.000	0.001	0.000	0.001	0.000	0.000	0.001	0.000	0.002	0.000	0.000	0.001	0.002	0.002
Fe^{+2}	0.001	0.004	0.004	0.000	0.002	0.003	0.003	0.002	0.003	0.006	0.004	0.002	0.003	0.003
Fe^{+3}	0.000	0.000	0.000	0.000	0.000	0.000	0.000	0.000	0.000	0.000	0.000	0.000	0.000	0.000
Cr	0.000	0.000	0.000	0.002	0.000	0.000	0.000	0.002	0.002	0.000	0.001	0.002	0.000	0.000
Al	1.359	1.287	1.355	1.289	1.136	1.327	1.311	1.307	1.243	1.341	1.336	1.173	1.256	1.083
Ti	0.000	0.000	0.000	0.000	0.000	0.002	0.000	0.000	0.000	0.001	0.000	0.001	0.000	0.001
Si	2.633	2.709	2.637	2.698	2.860	2.664	2.682	2.679	2.743	2.648	2.651	2.829	2.749	2.887
a_{An}	0.506	0.376	0.450	0.396		0.423	0.422	0.439						

Appendix Table 5b Representative electron-microprobe analysis of interior of plagioclase of charnockitic granulites.

Samples	90-66	90-61	90-30	90-29	90-58	90-62	90-48	90-36	90-56	90-34	90-54	90-46	90-52	90-57	90-47
Na_2O (wt %)	9.40	8.10	7.08	7.22	8.01	8.57	8.58	7.45	8.39	7.53	6.32	9.56	6.94	8.51	7.84
K_2O	0.26	0.23	0.19	0.16	0.15	0.16	0.54	0.16	0.21	0.21	0.33	0.27	0.53	0.19	0.48
CaO	4.09	6.04	7.47	7.65	6.32	5.86	5.50	7.29	6.71	7.44	9.13	3.72	8.34	6.31	6.70
MgO	0.00	0.01	0.00	0.00	0.07	0.01	0.00	0.00	0.00	0.00	0.01	0.01	0.00	0.07	0.01
MnO	0.00	0.00	0.01	0.01	0.03	0.00	0.00	0.00	0.04	0.00	0.03	0.00	0.00	0.00	0.00
FeO	0.05	0.13	0.04	0.07	0.11	0.03	0.05	0.06	0.05	0.07	0.05	0.07	0.11	0.05	0.05
Cr_2O_3	0.00	0.00	0.00	0.00	0.01	0.02	0.00	0.00	0.00	0.00	0.00	0.00	0.01	0.00	0.00
Al_2O_3	22.95	24.63	25.94	26.04	24.65	24.19	24.06	25.51	24.87	25.42	26.68	22.79	26.15	24.58	24.68
TiO_2	0.02	0.02	0.00	0.01	0.00	0.01	0.03	0.01	0.00	0.00	0.03	0.05	0.02	0.02	0.00
SiO_2	63.85	60.91	59.51	58.31	60.18	61.17	61.56	59.11	60.03	59.22	57.36	64.23	57.44	60.38	60.33
Total	100.62	100.07	100.25	99.46	99.55	100.02	100.32	99.58	100.29	99.90	99.93	100.70	99.54	100.12	100.09
Na (atoms)	0.801	0.698	0.611	0.629	0.695	0.739	0.738	0.647	0.725	0.653	0.550	0.841	0.608	0.736	0.677
K	0.015	0.013	0.011	0.009	0.008	0.009	0.031	0.009	0.012	0.012	0.019	0.015	0.301	0.011	0.027
Ca	0.193	0.287	0.356	0.369	0.303	0.279	0.262	0.359	0.320	0.357	0.439	0.175	0.404	0.302	0.320
Mg	0.000	0.001	0.000	0.000	0.005	0.001	0.000	0.000	0.000	0.000	0.001	0.001	0.000	0.005	0.001
Mn	0.000	0.000	0.000	0.000	0.001	0.000	0.000	0.000	0.001	0.000	0.001	0.000	0.000	0.000	0.000
Fe^{+2}	0.002	0.005	0.002	0.003	0.004	0.001	0.002	0.002	0.002	0.003	0.002	0.003	0.004	0.002	0.002
Fe^{+3}	0.000	0.000	0.000	0.000	0.000	0.000	0.000	0.000	0.000	0.000	0.000	0.000	0.000	0.000	0.000
Cr	0.000	0.000	0.000	0.000	0.000	0.001	0.000	0.000	0.000	0.000	0.000	0.000	0.000	0.000	0.000
Al	1.189	1.290	1.359	1.379	1.300	1.268	1.258	1.348	1.306	1.340	1.412	1.179	1.391	1.291	1.297
Ti	0.001	0.001	0.000	0.000	0.000	0.000	0.001	0.000	0.000	0.000	0.001	0.002	0.001	0.001	0.000
Si	2.806	2.707	2.646	2.620	2.692	2.721	2.731	2.649	2.675	2.649	2.576	2.818	2.593	2.690	2.689
a_{An}	0.234	0.390	0.503	0.506	0.412	0.365	0.336	0.354	0.415	0.482	0.588	0.206	0.533	0.391	0.429

Journal of Geological Society of Sri Lanka Vol. 16 (2014), 170-205
Professor P.G. Cooray Memorial Volume

Appendix Table 6a Representative electron-microprobe analysis of hornblende of charnockitic granulites.

Samples	90-70	90-73	90-76	90-69	91-14	90-43	B-108	B-109	90-49	90-41	90-68
Na_2O (wt %)	1.51	1.82	1.50	1.94	1.61	1.96	1.78	1.73	1.53	1.66	1.62
K_2O	1.38	2.05	1.54	0.93	2.29	1.96	2.12	1.85	1.64	2.08	1.20
CaO	11.42	10.81	11.13	9.84	10.62	10.69	10.75	10.59	10.87	10.94	11.19
MgO	10.17	4.42	10.27	11.69	0.48	6.45	6.08	6.09	7.60	4.50	8.97
MnO	0.54	0.07	0.14	1.26	0.95	0.13	0.14	0.10	0.26	0.17	0.30
FeO	17.89	26.58	17.79	17.02	31.32	23.64	23.37	22.96	21.27	24.48	19.44
Cr_2O_3	0.02	0.00	0.02	.0.02	0.00	0.04	0.03	0.00	0.00	0.09	0.01
Al_2O_3	10.59	10.38	11.20	10.09	10.40	10.87	10.26	10.22	11.17	10.81	10.57
TiO_2	1.51	2.73	2.17	1.65	1.97	2.13	2.22	2.22	2.44	2.41	1.78
SiO2	42.20	39.45	42.23	42.93	36.84	40.29	40.72	40.80	40.44	38.50	41.82
Total	97.27	98.30	98.00	97.37	96.48	98.16	97.47	96.57	97.23	95.65	96.90
Na (atoms)	0.440	0.556	0.433	0.551	0.519	0.586	0.539	0526	0.455	0.520	0.477
K	0.265	0.412	0.292	0.174	0.485	0.386	0.422	0.370	0.321	0.429	0.233
Ca	1.840	1.822	1.774	1.543	1.889	1.768	1.799	1.780	1.786	1.894	1.823
Mg	2.279	1.036	2.277	2.550	0.119	1.483	1.415	1.423	1.737	1.084	2.032
Mn	0.069	0.009	0.018	0.156	0.134	0.017	0.019	0.013	0.034	0.023	0.039
Fe^{+2}	1.559	3.096	1.503	0.570	3.892	2.472	2.746	2.680	2.059	3.144	1,846
Fe^{+3}	0.691	0.401	0.710	1.513	0.457	0.579	0.307	0.332	0.669	0.164	0.626
Cr	0.002	0.000	0.002	0.002	0.000	0.005	0.004	0.000	0.000	0.012	0.001
Al	1.878	1.927	1.965	1.742	2.037	1.978	1.890	1.891	2.020	2.060	1,895
Ti	0.171	0.323	0.243	0.182	0.246	0.247	0.261	0.262	0.281	0.293	0,204
Si	6.351	6.207	6.282	6.284	6.116	6.218	6.359	6.399	6.201	6.221	6.358

Note: structural formulae based on 13-Na, Ca, K

Appendix Table 6 b Representative electron-microprobe analysis of hornblende of charnockitic granulites.

Samples	90-52	90-57	90-46	90-34	90-56	90-61	90-29	90-58	90-62	90-36	B-117
Na_2O (wt %)	1.39	1.85	1.82	1.76	2.04	1.79	1.66	1.81	1.74	1.71	2.04
K_2O	1.49	2.19	1.43	1.96	1.94	2.04	2.15	1.86	1.80	2.02	1.82
CaO	11.09	10.89	10.38	1048	11.40	10.92	10.95	10.76	11.05	10.66	10.00
MgO	9.55	7.83	3.82	5.94	7.54	6.12	6.27	7.45	4.45	6.06	1.15
MnO	0.32	0.02	0.29	0.12	0.09	0.14	0.12	0.12	0.04	0.10	0.12
FeO	17.63	20.56	27.66	23.56	20.99	23.39	22.99	21.09	25.87	23.34	31.99
Cr_2O_3	0.00	0.06	0.01	0.03	0.06	0.00	0.00	0.06	0.00	0.01	0.00
Al_2O_3	11.61	10.66	10.06	10.87	10.84	10.19	10.65	10.58	10.17	10.75	9.04
TiO_2	1.69	1.91	1.99	1.99	2.30	2.21	1.70	2.11	1.78	2.13	2.01
SiO2	41.40	40.53	39.93	39.89	39.71	40.28	39.77	41.22	39.64	40.12	38.59
Total	96.17	96.51	97.38	96.61	96.89	97.08	96.22	97.06	96.55	96.89	96.75
Na (atoms)	0.410	0.559	0.557	0.535	0.618	0.545	0.509	0.542	0.539	0.519	0.648
K	0.289	0.435	0.288	0.392	0.387	0.409	0.434	0.366	0.367	0.403	0.380
Ca	1.804	1.817	1.755	1.761	1.910	1.838	1.855	1.781	1.894	1.788	1.756
Mg	2.161	1.817	0.898	1.388	1.757	1.433	1.477	1.715	1.061	1.414	0.281
Mn	0.041	0.003	0.039	0.016	0.012	0.019	0.016	0.016	0.005	0.013	0.017
Fe^{+2}	1.584	2.345	2.956	2.536	2.536	2.767	2.640	2.350	3.183	2.603	3.814
Fe^{+3}	0.655	0.333	0.695	0.554	0.209	0.306	0.400	0.374	0.278	0.453	0.570
Cr	0.000	0.007	0.001	0.004	0.007	0.000	0.000	0.007	0.000	0.001	0.000
Al	2.080	1.959	1.872	2.011	2.000	1.888	1.986	1.927	1.919	1.985	1.747
Ti	0.193	0.224	0.236	0.235	0.270	0.261	0.202	0.245	0214	0.251	0.248
Si	6.286	6.312	6.302	6.256	6.209	6.327	6.278	6.366	6.340	6.280	6.324

Note: structural formulae based on 13-Na, Ca, K

Journal of Geological Society of Sri Lanka Vol. 16 (2014), 170-205
Professor P.G. Cooray Memorial Volume

Appendix Table 7 Temperature (^0C) estimates from different garnet-pyroxene and two-pyroxene thermometers using mineral core compositions.

Samples	Cpx-Opx Wood & Banno (1973)	Cpx-Opx Lindsley (1983) °C	Grt-Opx Harley (1984) °C	Grt -Opx Sen & Bhattacharya (1984) °C	Grt-Cpx Ellis & Green (1979) °C
90-77	762	710	719	827	757
90-43	790	695	720	825	741
91-20	773	780	723	817	753
90-47	841	763	741	849	794
90-41	762	700			
90-54	801	757	751	860	737
90-34	780	725	712	818	751
90-56	742	695	740	855	771
90-66	688	630	709	822	.....
90-61	779	685	723	836	779
90-30	821	727	685	781	768
90-62	745	670	783	922	822
B-117			640	705	733
90-29			715	823	
90-58			659	744	
90-48			677	747	
90-36			715	822	
90-46			638	721	
90-52			784	895	
90-57			690	791	
91-20			723	817	753
90-49			662	740	
B-108			751	858	
B- 109			690	788	
90-70			803	925	
91-14					757
90-73					779

Appendix Table 8 Paleo-pressure estimates from garnet-pyroxene-plagioclase-quartz equilibria (at 800°C) using mineral core compositions.

Sample #	Bhattacharya et al. (1991) Grt+Opx+Pl+Qz	Perkins and Chipera (1995) Grt+Opx+Pl+Qz	Holland and Powell (1998) Data Set Grt+Cpx+Pl+Qz
90-61	8.0	8.4	8.0
90-30	7.3	8.0	7.4
90-29	7.1	7.8	-
90-58	8.2	8.9	-
90-62	8.0	8.5	8.0
90-48	8.8	9.8	
90-36	7.4	8.0	-
90-56	8.2	9.0	
90-34	7.1	7.8	7.6
90-54	7.5	9.0	7.7
90-46	9.3	9.6	-
90-52	8.4	10.8	
90-57	8.3	9.0	
90-47	8.5	9.9	9.2
91-20	8.0	9.8	9.3
90-49	8.5	9.9	
B-108	7.3	7.9	
B-109	8.0	8.6	
90-43	7.9	8.4	8.2
90-77	8.0	8.6	8.0
90-70	8.6	11.0	
B-117	9.9	10.1	9.6
90-66	7.8	8.3	8.5

Appendix Table 9 Mineral constituents of calc-silicate rock samples.

	Scp	Di	Pl	Wo	Cal	Grs	Qz	Gr	Spn*	Ves	Czo*
AJ-1	+	+	+	+	+	+	+	-	-	+	-
U-143	+	+	-	+	+	+	+	-	-	-	-
R-163	+	+	+	-	+	+	+	-	-	-	-
R-206	+	+	+	-	+	-	+	+	-	-	-
SAM-100	-	-	+	-	-	+	-	-	+		+

*accessory minerals

Table 10 Representative electron-microprobe analysis of scapolite and plagioclase from calc-silicate rocks.

Scapolite (Si +Al = 12)					Plagioclase (8 oxygen)				
Sample #	U - 143	R - 163	R - 206	AJ - 1	Sample #	SAM-100	R - 163	AJ-1	R-206
SiO_2 (wt %)	46.58	45.46	47.56	48.89	SiO_2	42.76	50.82	56.45	60.41
Al_2O_3	27.98	27.77	27.46	26.96	Al_2O_3	36.64	31.04	27.57	25.49
FeO	0.17	0.18	0.00	0.06	FeO	0.21	0.09	0.01	0.04
K_2O	0.34	0.48	0.22	0.47	K_2O	0.01	0.17	0.15	0.35
CaO	18.01	18.86	17.63	16.34	CaO	20.33	13.91	10.2	6.92
Na_2O	2.99	2.77	3.38	4.01	Na_2O	0.04	3.61	5.60	7.74
Cl	0.00	0.00	0.03	0.04					
Total	96.07	95.52	96.25	96.82	Total	100.01	99.64		100.5
Si (atoms)	7.03	6.98	7.14	7.320	Si	1.98	2.32	2.57	2.67
Al	4.97	5.02	4.86	4.680	Al	2.00	1.67	1.46	1.32
Fe^{+2}	0.02	0.02	0.00	0.005	Fe^{+2}	0.01	0.00	0.00	0.00
K	0.01	0.09	0.04	0.090	K	0.00	0.00	0.00	0.00
Ca	2.91	3.10	2.84	2.625	Ca	1.01	0.68	0.48	0.33
Na	0.87	0.82	0.98	1.166	Na	0.04	0.32	0.56	0.66
a_{Me}		0.30		0.15	a_{An}		0.75	0.60	
X_{Me}	77	79	74	69	X_{An}	100	68	46	33
An_{Eq}	66	68	62	56	X_{An}				33

Table 11 Representative electron-microprobe analyses of garnet and diopside from calc-silicate rocks.

	Garnet						Diopside				
Sample No.	SAM 100	U – 143 (porphyroblast)	U -143 (corona)	AJ –1	R - 163		U -143	R-163	AJ-1	U-143	R-206
SiO_2	37.58	38.61	38.8	38.55	38.65	SiO_2	51.75	49.86	50.97	51.55	51.88
Al_2O_3	19.27	20.06	20.46	21.09	19.91	Al_2O_3	1.16	1.7	0.69	0.68	0.88
TiO_2	0.56	0.74	0.24	0.32	0.44	TiO_2	0.02	0.13	0.05	0.02	0.06
FeO	9.57	0.93	0.33	0.56	3.55	FeO	10.39	15.96	14.73	12.34	8.35
Fe_2O_3	4.5	4.08	4.48	3.95	3.78	Fe_2O_3	1.48	1.43	0.33	0.82	0.78
Cr_2O_3	0.00	0.08	0.05	0.00	0.0	Cr_2O_3	0.03	0.00	0.00	0.00	0.03
MnO	0.33	0.48	0.45	0.27	0.42	MnO	0.44	0.29	0.12	0.27	0.2
MgO	0.06	0.30	0.17	0.16	0.26	MgO	10.36	6.71	7.89	9.9	12.46
CaO	27.6	35.04	35.54	35.71	32.93	CaO	24.45	23.5	24.18	23.88	24.37
Total	99.47	100.32	100.52	100.01	99.93	Total	100.08	99.58	99.20	99.38	99.01
Si	2.95	2.94	2.94	2.93	2.96	Si	1.96	1.95	1.98	1.98	1.95
Al	1.78	1.79	1.83	1.87	1.80	Al	0.05	0.07	0.02	0.03	0.04
Ti	0.03	0.04	0.01	0.02	0.03	Ti	0.00	0.00	0.00	0.00	0.00
Fe^{+2}	0.63	0.06	0.02	0.04	0.23	Fe^{+2}	0.33	0.5	0.48	0.4	0.25
Fe^{+3}	0.26	0.23	0.26	0.22	0.22	Fe^{+3}	0.04	0.07	0.01	0.02	0.04
Cr	0.00	0.01	0.00	0.00	o.00	Cr	0.00	0.00	0.00	0.00	0.00
Mn	0.02	0.03	0.03	0.02	0.03	Mn	0.01	0.01	0.00	0.01	0.00
Mg	0.01	0.03	0.02	0.02	0.03	Mg	0.59	0.40	0.46	0.57	0.7
Ca	2.32	2.86	2.89	2.88	2.71	Ca	0.99	0.99	1.01	0.98	0.99
a_{Grs}	0.85			0.85	0.70						
Prp	0.25	1.13	0.63	0.62	0.98	Wol.	52.1	52.3	51.8	50.3	50.0
Alm	21.2	1.98	0.72	1.19	7.61	Ens.	30.7	21.3	23.53	29.2	35.4
Grs	64.72	84.03	85.03	86.68	79.62	Fs.	17.2	26.4	24.64	20.5	14.6
Sps	0.73	1.04	0.97	0.58	0.90						
Adr		11.59	12.51	10.93	10.87						

Journal of Geological Society of Sri Lanka Vol. 16 (2014), 170-205
Professor P.G. Cooray Memorial Volume

National Digitization Project

National Science Foundation

Institute : National Science Foundation

1. Place of Scanning : Sanje (Private) Ltd, Hokandara
2. Date Scanned : 02/06/2017
3. Name of Digitizing Company : Sanje (Private) Ltd, No 435/16, Kottawa Rd, Hokandara North, Arangala, Hokandara
4. Scanning Officer

Name : Angelo Melvin Luwis

Signature : A. M. Luwis

Certification of Scanning

I hereby certify that the scanning of this document was carried out under my supervision, according to the norms and standards of digital scanning accurately, also keeping with the originality of the original document to be accepted in a court of law.

Certifying Officer

Designation : Information Officer

Name : Renuka Sugathadasa

Signature : R. P. Sugathadasa

Date : 02/06/2017

"This document/publication was digitized under National Digitization Project of the National Science Foundation, Sri Lanka"